The lithospheric mantle and lower crust-mantle relationships under Scotland: a xenolithic perspective

Journal Article

Citation:

Upton, B.G.J.; Downes,H.; Kirstein, L.A.; Bonadiman, C.; Hill, P.G.; Ntaflos, T. (2011)
The lithospheric mantle and lower crust-mantle relationships under Scotland: a xenolithic perspective –
Journal of the Geological Society 168(4), pp.873-886

The lithospheric mantle and lower crust/mantle relationships under Scotland: a xenolithic perspective

B.G.J. UPTON[1*], H. DOWNES[2], L. A. KIRSTEIN[1], C. BONADIMAN[3], P.G. HILL[1] & NTAFLOS T.[4],

1 *School of GeoSciences, University of Edinburgh, EH9 3JW, Edinburgh, U.K.*

2 *Department of Earth and Planetary Sciences, Birkbeck University of London, Malet Street, London WC1E 7HX U.K.*

3 Department of Earth Sciences, University of Ferrara, via Saragat 1, 44100 Ferrara, Italy.

4 Department of Lithospheric Research, University of Vienna, Althanstrasse 14, 1090 Vienna, Austria.

**Corresponding author (email: brian.upton@ed.ac.uk)*

Abstract: In the British Isles the majority of volcanic rocks containing upper mantle and lower crustal xenoliths occur in Scotland. Most of the occurrences are of Carboniferous-Permian age. This paper presents new data on the mineral chemistry of spinel lherzolite xenoliths from the five principal Scottish tectonic terranes. Compositional variations among the four principal minerals emphasize the broad lateral heterogeneity of the sub-continental lithospheric mantle across the region. The remarkable range of Al_2O_3 *vs* CaO exhibited by the clinopyroxenes demonstrates the extremely complex tectono-magmatic history of the Scottish lithosphere. The generalised age increase from southern and central Scotland to the older Northern Highland and Hebridean Terranes of the north and north-west, with concomitant complexity of geological history is reflected also by trace element and isotopic studies. Reaction relationships in lherzolites from the Hebridean Terrane, due to pervasive metasomatism, involve secondary growth of sodic feldspar. This, and light REE-enrichment of clinopyroxenes points to involvement of a natro-carbonatitic melt.

Most pyroxenitic xenoliths are inferred to have formed as cumulates from underplating magmas, forming a basal crustal layer with a generally sharp discontinuity above the underlying (dominantly lherzolitic) mantle. A second discontinuity is inferred to separate these ultramafic cumulates from overlying, broadly cognate meta-gabbroic cumulates.

Xenoliths of upper mantle and lower crustal origin occur over a wide area of the British Isles but are most abundantly represented in Scotland. There, some seventy xenolith localities are distributed in a crudely arcuate pattern that embraces a) southern and central Scotland (the Palaeozoic Southern Uplands and Midland Valley Terranes), b) the western sides of the Proterozoic Grampian Terrane (between the Highland Boundary Fault and the Great Glen Fault), c) the western and north-eastern margins of the Northern Highland Terrane (bounded by the Great Glen Fault and the Moine Thrust), d) the Archaean-Palaeoproterozoic Hebridean Terrane west of the Moine Thrust. Thus material from beneath all five of the major tectonic terranes can be sampled (Fig. 1). Almost all of the hosts (basanites and other sub-silicic mafic rocks) are of late Palaeozoic age (lower Carboniferous to Permian) with the exception of a dyke near Loch Roag, Outer Hebrides (Hebridean Terrane) dated at c. 47 Ma (Menzies *et al.*, 1988; M. Timmerman, pers. com.).

Fig. 1 about here.

The generalised age increase of the shallow crust from SE to NW across Scotland probably reflects that of the deeper crust and lithospheric mantle (Menzies & Halliday, 1988; Macdonald & Fettes, 2007). Furthermore, the composition of the sub-continental lithospheric mantle (SCLM) may itself be broadly related to the tectonic-thermal age of the overlying crust (Griffin *et al.*, 2009).

Previous accounts of the Scottish SCLM have largely concerned their geochemistry, focussing on incompatible elements and isotopic characteristics (Menzies *et al.*, 1987; Menzies *et al.* 1988; Menzies & Halliday, 1988; Long *et al.*

1991: Downes *et al*., 2001; 2007; Bonadiman *et al.*, 2008.) These accounts have drawn attention to the extensive lateral chemical heterogeneity in the SCLM as represented by mantle xenoliths. The last petrological overview of the Scottish SCLM was compiled over twenty years ago (Hunter & Upton, 1987). The present paper considers how this heterogeneity is reflected in the mineral chemistry of the spinel lherzolite xenoliths from thirteen localities distributed across the five tectonic terranes. It presents new data on the spinel lherzolites, considers the implications of previous geochemical studies and discusses the probable relationships between the mantle and crust.

Late Palaeozoic extensional tectonics affecting Scotland led to widespread intraplate mafic volcanism typified by the OIB-type geochemistry common to such (typically) alkalic basaltic provinces (Smedley, 1988; Wallis, 1989; Upton *et al*., 2004; Kirstein *et al*., 2006). Carboniferous volcanism in central Ireland, northern England and southern Scotland represents one of the earliest, if not *the* earliest, examples of this type of province, as exemplified by the Basin and Range, Pannonian Basin and the Massif Central, that was to become globally widespread throughout Mesozoic-Cenozoic times. These occurrences also provide very early instances of xenoliths hosted by alkali basaltic (basanites grading to olivine melanephelinitic types) rather than by kimberlite, carbonatite, lamproite or ultramafic lamprophyre magmas. This non-uniformitarian phenomenon has implications for the thermal history and the evolution of the continental lithosphere at large.

With regard to with the metamorphic zonation imposed during the peak of the Caledonian Orogeny (~460 Ma), the late Palaeozoic xenolith localities in Scotland tend to lie around the low-temperature isotherms, with basanitic magmatism (and associated xenoliths) being absent within the higher-temperature metamorphic zones.

Lithospheric composition, temperatures, thickness and pre-existing structures may have an important control in this geographic distribution. Woodcock and Strachan (2000) noted that geophysical studies of the upper mantle beneath the British Isles suggest that in some areas the main mantle fabrics may lie parallel to Caledonian and Variscan structures in the overlying crust.

The modal distribution of xenolith types at individual localities is also instructive. Some occurrences yield a wide spectrum of xenoliths, representing both mantle and lower crustal rock types but at others the compositional range is more restricted. Thus at some, peridotite appears to be the sole rock-type whilst at others only pyroxenitic ± meta-gabbroic xenoliths occur.

The xenoliths are typically small (<30 mm) so that composite xenoliths are rare. Apart from scarce quartzo-feldspathic xenoliths of (assumed) mid-crustal derivation (<20 km depth), most fall into one of the following categories: a) peridotitic, with metamorphic fabrics, b) pyroxenitic (*sensu lato),* including wehrlites, olivine clinopyroxenites, clinopyroxenites, websterites grading to orthopyroxenites, and metasomatised varieties such as biotite- and pargasite/kaersutite pyroxenites grading to glimmerites or hornblendites and c) meta-gabbroic to meta-dioritic xenoliths, typically possessing granulite-facies fabrics ('mafic granulites'). Most of the pyroxenitic (s.l.) and mafic xenoliths are inferred to have originated as cumulates from basaltic magmas (e.g. Upton *et al*., 1983; Halliday *et al*., 1993; Downes *et al.* 2007). Data from several well-studied Scottish xenolith suites point to a generalised genetic relationship between the pyroxenites and mafic granulites. Although some of the pyroxenites may have crystallised within the upper mantle, the majority are considered to be representative samples of the deepest crustal layers (Downes *et al*.,

2001; Downes *et al.*, 2007; Upton *et al*., 1998 and 2001). This conclusion is supported by fluid inclusion studies (Kirstein *et al*., 2004).

Despite the inference that many of the pyroxenitic xenoliths originated as cumulates, some may have been generated by metasomatism of peridotitic protoliths (*cf*. Meen, 1987) as has been argued by Menzies and Halliday (1988). The very scarce garnet pyroxenite xenoliths are mainly confined to the Midland Valley (Upton, *et al*., 2003) and are regarded as high-pressure (~20 kbar) crystallisation products of alkali basalt magmas.

Mantle peridotites

The Scottish mantle xenoliths almost exclusively comprise spinel lherzolite, the commonest of all mantle-derived rocks found in xenoliths and orogenic peridotite bodies and stable to depths of 55-60 km (Griffin & O'Reilly, 1987a). Although traditionally considered as restitic (Dick & Bullen, 1984; Arai, 1994), the lherzolites may, alternatively, represent re-fertilised products of previously depleted harzburgitic rocks (Bodinier *et al*., 2008; Griffin *et al*., 2009).

Whereas true harzburgite xenoliths are unknown from Scotland, clinopyroxene is scarce in the most depleted lherzolites (e.g. at Oldhamstocks in the Southern Uplands terrane). The lherzolites exhibit granoblastic to porphyroclastic textures, with rare flaser textures. Olivines are typically 10-100 micron diameter whilst orthopyroxene porphyroclasts can attain 10mm. The Scottish lherzolite xenoliths tend to be finer-grained in comparison with others on a global basis (B.E. Tabor, pers.com.), possibly due to cataclastic deformation during Caledonide tectonism with a lack of subsequent annealing by the late Palaeozoic.

Rare late-stage phlogopite or pargasite in the lherzolites denotes overt or modal metasomatism (Alexander *et al*., 1986; Hunter & Upton, 1987). Whilst chrome-diopside and spinel typically appear unaltered, olivines and orthopyroxenes have commonly experienced alteration to serpentine minerals or carbonate and at only a few localities are the peridotite xenoliths substantially pristine.

Representative analyses for olivines, orthopyroxenes, clinopyroxenes and spinels are presented in Tables 1 & 2. Analyses of feldspar are given in Table 3. Electron microprobe analyses were carried out at four laboratories. In Edinburgh, the instrument used was a Cameca SX100, equipped with 5 x wavelength dispersive (WD) spectrometers. It was operated at a gun potential of 20 kV and a probe current (as measured with a Faraday Cup) of 20 nA. Counting times on the elements were 20 seconds on both peak and background. Elemental calibration was made against a set of well-established standard materials. The instrument used at the Istituto di Geoscienze e Georisorse in Italy was a Cameca Camebax equipped with 4 x WD spectrometers. The gun potential used was 15 kV with a current of 20 nA. 100 second count times were used for analysis. At the Vrije Universiteit, Amsterdam, a JEOL JXA-8800M electron probe was used with a 15 kV accelerating voltage and 25 nA current. In Vienna the equipment was a Cameca SX100 with 4 WDS and an EDS. An accelerating voltage of 15 kV with a 20 nA focused beam current and a 20 second counting time on peak positions were used for routine analyses. For feldspars, a 5 micron defocused beam current and a counting time of 10 seconds for Na and K were used. For trace element analysis in olivine (Al, Cr, Ti, Zn, P) the applied conditions were: accelerating voltage 20 kV, beam current 150 nA and counting times of 150 and 100 seconds on peak and background positions respectively. Detection limits were: Al, 15ppm; Ti, 29 ppm; Ca, 26 ppm; Ni, 79 ppm; Mn, 55 ppm, Cr, 33 ppm; Zn, 55

157 ppm; P, 43 ppm). Matrix corrections on all instruments were made by the proprietary
158 PAP software supplied by the manufacturer of the instruments
159
160 *Table 1 about here*
161 **Olivines**
162 The olivines range from Fo_{91} to Fo_{87} with the majority clustering around Fo_{89}
163 (Table 1), as is typical for spinel lherzolites globally (*cf*. Basaltic Volcanism Study
164 Project, 1981). Spinel lherzolites have, until recently (Bodinier *et al*., 2008; Griffin *et*
165 *al*., 2009) been regarded as restites that have undergone variable depletion as a
166 consequence of Proterozoic or early Palaeozoic melt extraction events. A MgO *vs*.
167 NiO wt% plot for the olivines is shown in Fig.2. The data are unfortunately limited
168 because in most samples the olivines have been pseudomorphed. The diagram shows
169 MgO contents from 48 to 51 wt% and NiO from 0.33 to 0.45 wt% for the majority of
170 the analyses, mostly within the normal ranges for mantle olivines (McDonough &
171 Rudnick, 1998). Some, however, particularly from Rinibar have NiO contents <0.3
172 wt% (Table 1), possibly related to metasomatism as reported by Bonadiman *et al*.
173 (2008).
174
175 *Fig. 2 about here (MgO vs. NiO, olivines)*
176
177 CaO contents of the olivines are generally <0.07 wt% with higher values (>0.1
178 wt%) from Streap Com'laidh (Northern Highland Terrane), Hexpath & Oldhamstocks
179 (Southern Uplands Terrane) and especially in some of the Ruddon's Point and Fidra
180 (Midland Valley Terrane) xenoliths (0.11 – 0.20 wt%). Olivine Cr_2O_3 contents are

typically 0.01-0.02 wt% but higher values (up to 0.05 wt%) are found in the Cooms Fell and Oldhamstocks lherzolites (both from the Southern Uplands Terrane).

The sub-Hebridean lithospheric mantle was shown to be highly enriched both isotopically and in light rare-earth elements (LREE) (Menzies *et al.*, 1987; Menzies & Halliday, 1988; Long *et al.*, 1991). Accordingly a special attention was given to analysis of trace components in the olivines from Loch Roag. Al, however, is close to the detection limit (25 ppm), Ti and P lie below the detection limit (25 ppm), with Zn of ~60 ppm. The Cr level is < 0.01 wt. %. Thus none of these values suggests any enrichment.

Fig 3 about here.

Spinels

Spinel compositions vary widely: although most have Cr# values (Cr/(Al + Cr)) <20, these can be up to ~70 (Table 1). Fig. 3 depicts the relationship between Cr# (spinel) and Mg# (olivine) in relation to the ol-sp mantle array (Arai, 1987; 1994). Most data fall into the lower Cr# (<0.30) - lower Mg# field, suggesting that the peridotites are relatively undepleted. However, spinels from Riska (Northern Highlands) and some from Cooms Fell (Southern Uplands) have higher Cr# denoting greater degrees of melt depletion. Whilst the Rinibar (Orkney, Northern Highland Terrane) and Loch Roag (Hebridean Terrane) compositions lie both within and outside the field boundaries, all have the comparatively high Cr# values indicative of greater degrees of depletion (Arai, 1994). Spinel data (Cr# vs. Mg#) for the lherzolite spinels (Fig. 4) support the conclusion that many xenoliths, including those from Colonsay (Grampian Terrane) and Streap Com'laidh (Northern Highland) samples,

have experienced only relatively small degrees of melt extraction in contrast to those from Machrihanish (Grampian Terrane) and many of those from Rinibar (Northern Highland). The forsterite content can be significantly changed as a result of metasomatism by incompatible-element-rich fluids and can be shifted off the ol-sp mantle array towards lower Fo values (Irving, 1980; Goto & Arai, 1987). Accordingly metasomatism may be the explanation for those Rinibar and Loch Roag samples lying to the right of the array (Fig. 4).

The Loch Roag spinels are distinctive compositionally in having lower MgO contents (15-13 wt% as opposed to 21-17 wt% in the other spinels studied) and in having higher TiO_2 (~0.33 wt% *vs*. <0.18 elsewhere). Their Cr_2O_3 (49-35 wt%) are also relatively high, the majority of the other lherzolite spinels containing <20 wt% Cr_2O_3. There is notable within sample variability as shown in sample LR81, with spinels having Cr # 42.12 and 67.13 (Table 1b). Texturally the Loag Roag spinels are unique among the Scottish xenoliths studied in that they have undergone a reaction in which sodic feldspar was produced.

Fig. 4 about here. (Cr# vs. Mg#, spinels)

Clinopyroxenes

Clinopyroxene is, along with spinel, the phase least affected by secondary alteration. The relationship between CaO and Al_2O_3 (Fig. 5) also provides an indication of depletion, the more aluminous (>5 wt% Al_2O_3) clinopyroxenes being the least depleted. The clinopyroxenes show a broad 'tail' towards lower Al_2O_3, including those from Oldhamstocks, Ruddon's Point, Machrihanish, Riska and many from Rinibar, that may reflect increasingly refractory character. An increase in Cr_2O_3 and

NiO also monitors the increasing degree of refractoriness (McDonough & Rudnick, 1998). NiO is typically less than 0.06 wt. % but rises to ~0.09 wt% in the Cooms Fell lherzolites. Generally Cr_2O_3 in the clinopyroxenes ranges between 0.4-0.7 wt% but notably higher values (>1.00 wt%) are found in Riska, Streap Com'laidh and Cooms Fell lherzolites but with the highest values (up to 1.7 wt%) at Oldhamstocks.

Clinopyroxenes from the Loch Roag samples are noteworthy in being more siliceous (~ 54 wt% SiO_2) than elsewhere in Scotland (51-52 wt%), with significantly higher sodium contents (2.56 – 2.32 wt% Na_2O compared to 2.0 – 0.8 wt% at other localities) (Table 2). They tend also to be comparatively poor in Al_2O_3 (4.7-4.2 wt% Al_2O_3) whereas most of the other lherzolite clinopyroxenes contain 8-5 wt%.

Fig. 5 about here (Ca vs. Al_2O_3 in cpxs))

Orthopyroxenes

TiO_2 values of the orthopyroxenes are mostly <0.12 wt% but are particularly low (below detection) at Oldhamstocks (Table 2). Al_2O_3 typically falls between 2.0 – 4.6 wt%, rising to ~5.38 wt% at Cooms Fell. The Loch Roag orthopyroxenes are relatively Al-poor (2.6 - 2.2 Al_2O_3 wt%) in comparison with values >3 wt% for the majority of orthopyroxenes from other localities. CaO values generally fall into the range 0.3 – 0.8 wt% but the Oldhamstocks orthopyroxenes are notably more calcic (~0.98 CaO wt%) as well as being very poor in TiO_2 (Table 2).

Experimental and theoretical studies concerning peridotite melting provide depletion trends in the form of modal abundances and mineral compositions. With increasing degrees of depletion, the modal proportion of olivine increases whilst those of orthopyroxene, clinopyroxene and spinel decrease. Since Al, Ca, Na, K and Ti are

256 more incompatible during melting than Mg, Cr and Ni, their concentrations are
257 highest in the least depleted peridotites. On the basis of the mineral proportions of the
258 depleted-MORB mantle (DMM) proposed by various authors (e.g. Johnson *et al*.,
259 1990, Baker & Beckett, 1999, Workman & Hart, 2005 and references therein)
260 resulting from progressive melt extraction from primitive upper mantle (PUM;
261 McDonough & Sun, 1995), we calculate the major element compositions and
262 proportions of the primitive source, assuming pressures and temperatures within the
263 spinel stability field. Using this simple model we model the melting curve for two
264 crucial elements (Al and Mg) in both ortho- and clinopyroxenes. The orthopyroxenes
265 of the Scottish peridotites broadly correspond to the hypothetical melting trend (Fig.
266 6), with the Riska and Oldhamstocks lherzolites, from the Northern Highland and
267 Southern Upland Terranes respectively, representing the most refractory mantle
268 domains. The Fidra orthopyroxenes show anomalously low values of MgO (30.5 –
269 32.5 wt%).
270
271 *Fig.6 about here (MgO vs. Al_2O_3 for opxs)*
272 The same melting curve calculated for the clinopyroxenes (Fig. 7) shows that, for
273 most of the xenolith population, this phase does not reflect the same degree of melting
274 as the coexisting orthopyroxenes. Therefore we have to postulate another process. In
275 terms of the major element compositions of the pyroxenes, only the Riska and
276 Oldhamstocks xenoliths appear to represent residues after extensive melt extraction.
277 In general, however, the clinopyroxenes cannot be described as resulting as residua
278 from simple melting. Clinopyroxenes from Ruddon's Point and Corrie na Ba have
279 particularly high Al_2O_3 contents, a characteristic considered to have come about from
280 metasomatism involving Al-rich melts (Bonadiman *et al*., 2008).

281

282 *Fig. 7. about here (MgO vs. Al_2O_3 for cpxs)*

283

284 **Feldspars**

285 The Loch Roag spinel lherzolites are unique among the samples studied in that
286 corroded spinel rims are bounded by anorthoclase and greenish Na-rich clinopyroxene
287 symplectite reaction rims. This mineral pair occurs along the sp-cpx, ol-ol and ol-cpx
288 contacts (Hunter & Upton, 1987). The feldspar has 9.64-9.38 wt% Na_2O and 0.33-
289 0.94 wt% K_2O (Table 3).

290

291 **Isotope and trace element data**

292 Apart from a few lherzolite xenoliths that have experienced modal metasomatism that
293 generated secondary pargasite (Black Rocks (Midland Valley Terrane; Alexander *et*
294 *al*., 1986), phlogopite (Riska, Northern Highland Terrane) and sodic feldspar (Loch
295 Roag, Hebridean Terrane), variable cryptic metasomatic enrichment has been inferred
296 from incompatible element and isotopic data, particularly in the Northern Highland
297 and Caledonian Foreland terranes (e.g. Menzies & Halliday, 1988). Such geochemical
298 signatures signify marked provinciality within the lithospheric mantle a generalised
299 decrease in enrichments from the Foreland Terrane SCLM in the NW to that beneath
300 distinctly younger crust under the Midland Valley in the SE (Fig. 8).

301

302 *Fig 8 about here (Nd vs. Sr data)*

303

304 Studies of the Loch Roag xenoliths have shown that the Hebridean Terrane is
305 underlain, at least locally, by lithospheric mantle marked by extreme chemical and

isotopic heterogeneity (Menzies *et al*., 1987; Menzies & Halliday, 1988; Menzies *et al*., 1988; Long *et al*., 1991). The metasomatising agents were deduced to have been carbonatitic melts, of probable asthenosphere origin (Long *et al*., 1991).

Mantle xenoliths from Rinibar (Orkney) record two distinct metasomatic styles, due to a) carbonatitic and b) more silicate-rich (kimberlitic) melts (Bonadiman *et al*., 2008). These melts were inferred to have derived from different degrees of partial melting of the same source, at 550 ± 50 Ma, when both Canadian and Finnish cratons were experiencing carbonatitic and kimberlitic magmatism and at a time when the Rodinian supercontinent was undergoing the break-up that ultimately resulted in formation of the Iapetus Ocean. Attendant on the subsequent Silurian to Devonian closure of Iapetus, fluids/melts from subducting slabs are believed to have affected the overlying mantle wedge and the lithospheric mantle. Such subduction-related modifications are recorded in mantle xenoliths from Streap, towards the south-western extremity of the Northern Highland Terrane (Menzies & Halliday, 1988; Bonadiman *et al*., 2008). The lack of a comparable subduction-related signature in the Orkney xenoliths emphasizes the regional variation in metasomatic history of the lithospheric mantle in northern Scotland. At all localities where radiogenic isotope ratios have been measured, $^{143}Nd/^{144}Nd$ varies between 0.1524 and 0.5131 except at Loch Roag in the Hebridean Terrane. $^{87}Sr/^{86}Sr$ is consistently higher in whole-rock vs. clinopyroxene analyses (Fig.8).

The SCLM beneath the Midland Valley and Southern Upland Terranes appear to have been little affected by metasomatic processes. These mantle xenoliths have isotopic characteristics akin to those of OIB-source mantle (Figure 8) and closely resemble the relatively depleted lithospheric mantle that underlies the Basin and Range, Eifel and Massif Central (Downes, 2001). The Midland Valley experienced

intraplate extensional magmatism in the late Palaeozoic and the crustal thinning and enhanced heat-flow may have accompanied asthenospheric upwelling, with concomitant lithospheric modification (Menzies & Halliday, 1988; Downes *et al*., 2001; Downes *et al*., 2007). It may be speculated that lithospheric delamination or erosion may have intervened during the period ~400-350 Ma, leaving a relatively youthful Midland Valley lithosphere that was unaffected by the long-term metasomatic modifications that affected the lithospheric mantle beneath the northern terranes.

The heterogeneity of the Scottish mantle peridotites is also reflected in the chondrite-normalised rare-earth element (REE) patterns of the clinopyroxenes (Fig. 9). None of the clinopyroxenes represent a simple melting trend and all are interpreted as being "secondary", resulting from extensive melt interaction. The light-REE convexity ($La_N<Ce_N$) may have resulted from crystallisation of the clinopyroxene from a primitive basaltic melt or, alternatively, from long-term-interaction between the clinopyroxenes and a metasomatic melt. The latter alternative appears more plausible.

The clinopyroxenes fall into different groups, according to the patterns of REE enrichment (Fig. 9). In one group, represented by clinopyroxenes from Rinibar, (Orkney) the patterns are strongly fractionated with a tendency to be concave-down in their $LREE_N$, with a fall from Ce to La. The relatively low $HREE_N$ values suggest that this clinopyroxene group originally equilibrated with garnet. Subsequent uplift of the mantle domain may have caused progressive destabilisation of the garnet and growth of spinel, redistributing the garnet REE budget between cpx and opx. Considering the HREE cpx/opx distribution coefficient (*ca.* 1; GERM online data bank), the 'new' cpx HREE profiles become less steep (although still fractionated).

In another group, clinopyroxenes that always have been in equilibrium with spinel have almost flat or negative fractionated HREE patterns (Simon *et al*., 2008). The fertile character (high Al_2O_3 contents) and the LREE-enriched to flat chondrite-normalized MREE-HREE profiles of the Streap and Fidra pyroxenes may denote long-term equilibration between lithospheric mantle in the spinel stability field and metasomatic melts related to subduction. Clinopyroxenes from Loch Roag lherzolites are characterised by flat normalised patterns other than in the LREE where there is strong enrichment from Sm to La (*cf*. Menzies & Halliday, 1988). Clearly several distinct metasomatic processes have affected the Scottish lithospheric mantle in time and space.

The meta-gabbroic (mafic granulite) xenoliths from Streap, Fidra and Loch Roag, also record highly radiogenic Sr (Menzies *et al*., 1987; Downes *et al*., 2001) and represent shallow sub-arc lithospheric mantle that was variably contaminated by fluid/melts related to subduction (Upton *et al*., 1999; Downes *et al*., 2001, Bonadiman *et al*., 2008). This is confirmed by the range of fluid inclusion densities in the Streap xenoliths with low- (0.78-0.82 g cm^{-3}), high- (~ 1 g cm^{-3}) density and super-dense (~1.17 g cm^{-3}) inclusions observed indicating fluids trapped at subcrustal depths (Kirstein et al., 2004).

Fig.9 about here

Pyroxenitic xenoliths

Many of the ultramafic xenoliths fall into the category of the globally widespread Type 2 xenoliths (Frey & Prinz, 1978), considered to be high-pressure (10–8 kb) cumulates from underplated mafic magmas (*cf*. White, 1966; Upton *et al*. 2001). Although in a few cases, ultramafic xenoliths interpreted as cumulates include

dunites, the majority of these Type 2 xenoliths contain aluminous augitic pyroxene. Since pyroxene is commonly the dominant component, the xenoliths will collectively be referred to as pyroxenites (*s.l.*). Most are wehrlites, olivine pyroxenites and clinopyroxenites, but websterites occur and, with increasing modal orthopyroxene, grade towards orthopyroxenites (Downes *et al*., 2007).

Mineral data for pyroxenite assemblages are presented in Hunter & Upton (1987), Upton *et al*. (1998), Upton *et al*. (2001) and Downes *et al*. (2007). The Mg# values are lower than in the mantle peridotites and the olivines typically range from Fo_{87-72}. In some, feldspar is a minor component, occurring either as an intercumulus phase or as feldspathic schlieren, with compositions ranging from bytownite to oligoclase and anorthoclase. Pargasitic to kaersutitic amphibole is common in some localities, occurring as oikocrysts in igneous-textured pyroxenites or in a replacive mode. Biotite is also common and gradation to glimmerite may have occurred through metasomatic introduction of Fe, Ti, K and H_2O to pyroxenitic and dunitic cumulates (*cf*. Lloyd, 1981). Spinels (hercynite to magnetite) are ubiquitous and ilmenites, commonly geikelite-rich, also occur. Some xenoliths appear to be clinopyroxene-hercynite cumulates. Although apatite is usually insignificant, it is present to several modal percent in some biotite clinopyroxenites.

Although the textures are typically metamorphic, some xenoliths retain igneous textures. These include wehrlites and olivine clinopyroxenites with clinopyroxene oikocrysts enclosing early olivines, websteritic types with poikilitic clinopyroxene around orthopyroxene, and hornblende pyroxenites with kaersutite oikocrysts enclosing clinopyroxenes (Upton *et al.*, 2001; Downes *et al*., 2007). In these the oikocrysts pseudomorph former intercumulus melt pores between cumulus olivine, orthopyroxene and clinopyroxene respectively. Some pyroxenitic xenoliths

have been found with intercumulus devitrification products indicating that they were still above their solidus temperatures at the time of entrainment, implying a genetic relationship to their host basanites.

Pargasite-bearing pyroxenites from Orkney, Duncansby Ness and Gribun (Mull) are regarded as metasomatic products from anhydrous pyroxenites, produced by influx of hydrous melts rich in Ca, Fe, Ti and K, as well as LREE, Zr, Nb, Y Ba and Sr (Upton *et al*., 1998; 2001). In extreme cases, the metasomatism culminated in production of hornblendite. Differences in pyroxenitic suites from localities only a few kilometres distant, (e.g. from Gribun and Fionnphort, Isle of Mull), show that such metasomatism can be highly localised (Faithfull & Upton, 2006).

Although the majority of the pyroxenitic xenoliths appear to have originated as cumulates, some may be metasomites derived from mantle peridotites. Thus, some wehrlitic and olivine clinopyroxenitic xenoliths from Loch Roag were considered to have resulted from metasomatic reaction between carbonatitic melts and anhydrous peridotite (Long *et al*., 1991).

Meta-basic xenoliths

Meta-gabbroic, dioritic and anorthositic xenoliths, common in all five terranes, have the characteristics of the 'mafic granulites' widely regarded as composing the continental lower crust (Rudnick, 1992; Downes, 1993). The majority are regarded as having formed as plagioclase-clinopyroxene cumulates from magmas undergoing fractional crystallisation and assimilation processes (Halliday *et al*., 1993). Equilibration pressure estimates of 8–6 kb for lower crustal xenoliths from Bute in the western Midland Valley (Downes *et al*. 2007) agree with the other indictors of relatively thin crust. Model ages, mineral ages and scattered whole-rock isochrons

suggest that precursors to the meta-gabbroic xenoliths were formed and metamorphosed in late Proterozoic and early Palaeozoic arc terranes during the Caledonian orogeny.

There is a remarkable overall compositional uniformity in the meta-gabbroic and meta-dioritic xenoliths across all the terranes, average SiO_2, Al_2O_3 and MgO contents being similar despite variation at any one locality. This uniformity implies that relatively reproducible processes of assimilation and crystallisation accompanied underplating by mafic magmas. Such underplating may have repeatedly exploited a density plane separating ultramafic cumulates from overlying feldspathic cumulates, thereby maintaining the overall structure of the lower crust (Cox, 1980; Halliday *et al*., 1993; Upton *et al*., 2001).

Crust-mantle relationships

Most of western Europe is underlain by thinner, warmer and less depleted lithosphere than that beneath the East European craton to which it was accreted (Gee & Stephenson, 2006). New crust is thin and of relatively low density but with cratonisation it gets thicker and denser and the crust/mantle boundary tends to become more poorly defined (Drummond & Collins, 1986). Whereas the thickness of the Scottish lithosphere is poorly constrained, it would appear probable that it thickens and increases in age and complexity, as traced north-westwards from the Midland Valley towards the Outer Hebrides (Menzies & Halliday, 1988).

Pyroxenitic dykes within the upper mantle may have provided some of the pyroxenitic xenoliths (*cf*. Wilshire & Shervais, 1975; Irving, 1980; Wilshire & Pike, 1975; Downes, 2007). However, the observation that pyroxenites occur in abundance at several Scottish localities where peridotites are rare or absent, implies that, at least in

457 those instances, they derive from sources that were not intimately associated with
458 lherzolites. We infer that the majority of the pyroxenitic xenoliths come from a (thick?)
459 ultramafic cumulate layer overlying the lherzolitic mantle and that they are themselves
460 overlain by the feldspathic (meta-gabbroic) cumulates. We regard the pyroxenitic
461 cumulates as higher-temperature magmatic products complementing the meta-gabbroic
462 cumulates much as the ultramafic basal units of large mafic intrusions do to the
463 overlying gabbroic cumulates, and that the ultramafic and mafic cumulate assemblage
464 jointly constitutes the lower crust (Upton *et al.,* 2001). Sub-horizontal boundaries
465 between the mantle lherzolites and the pyroxenitic cumulates and between the latter and
466 the meta-gabbroic cumulates are envisaged. The lower crust has long been considered
467 as consisting largely of layered igneous intrusions (e.g. Singh and McKenzie, 1993) and
468 the seismically-determined multiple layered reflectors within the mantle lithosphere
469 beneath northern Scotland (Ascencio *et al*., 2003) are probably due to layering within
470 the cumulates.

471 The concept of a 'petrological Moho', marked by the discontinuity between
472 tectonised peridotitic mantle and overlying ultramafic cumulates forming the base of
473 the oceanic crust was introduced by Greenbaum (1972) and Lippard *et al*. (1986). The
474 term was used to distinguish the discontinuity between what were interpreted to be
475 restite and cumulate facies from the seismic or geophysical Moho marking the
476 boundary between ultramafic and mafic rocks. Accordingly, the seismic Moho does
477 not necessarily coincide with the base of the crustal sequence and may well lie
478 significantly above it.

479 Cox (1980) postulated that the base of the continental crust comprises
480 ultramafic cumulates overlain by gabbroic cumulates, both products of underplating
481 magmas. He suggested that a single pulse of (picritic) magma along, or close to, the

crust-mantle boundary would differentiate into an upper gabbroic and a lower ultramafic layer, thus generating a new seismic Moho at the interface. Repeated injection along the new Moho would then regenerate gabbroic cumulates above while augmenting the ultramafic cumulates below. Such a discontinuity between tectonised mantle peridotites and overlying pyroxenite cumulates can be considered as analogous to the 'petrological Moho' (Lippard *et al*., 1986; Griffin and O'Reilly, 1987b), whilst that between the pyroxenitic and gabbroic zones represents the seismic Moho (Upton *et al*., 2001; Faithfull & Upton 2006). There is commonly a simple overall structure in layered mafic-ultramafic intrusions in which gabbroic cumulates overlie, more or less abruptly, ultramafic cumulates. Our observations are compatible with a model in which a crustal sequence of ultramafic (pyroxenitic) cumulates underlies the mafic cumulates.

There is a general acceptance that the continental seismic Mohorovičić Discontinuity marks the break from intermediate or basic crustal rocks to underlying ultrabasic rocks (Ringwood, 1975). Whilst the latter are frequently assumed to be 'normal' peridotite, this ignores the xenolithic evidence that pyroxenites can play a significant role in the lithospheric structure and suggests that the inferred 'sharp' transition from ultramafic to mafic cumulates may be erroneously identified as the crust-mantle boundary.

Discussion and Summary

The mineral chemistry of the Scottish spinel lherzolites clearly implies considerable variation in the degree to which they have undergone melt extraction whereas the distinctive mineral chemistry of the Loch Roag lherzolites, together with the presence of alkali feldspar reflects the metasomatism demonstrated by the LREE

and isotopic enrichment documented by Menzies *et al*., (1987), Menzies & Halliday, (1988) and Long e*t al*., (1991). The remarkable variation in Al_2O_3 in the clinopyroxenes compared to that in individual continental xenolith provinces (Fig. 5) may be attributable to the degree to which the extremely complex magmatic history of Scotland (Macdonald & Fettes, 2007) has left its imprint on the lithospheric mantle.

The sub-Scottish lithosphere exhibits an overall increase in age (and probably thickness) north-westwards beneath the Caledonides to the Archaean/Palaeo-Proterozoic Terrane. Greater age provided greater opportunities for the lithospheric mantle to be affected by migrating melt fractions, including those of probable asthenospheric origin as well as others from subducting oceanic lithosphere. These processes conferred ever greater complexity. LREE-enrichment through carbonatitic metasomatism within the cratonic lithosphere of the north-west. Carbonatite-mantle interaction, inferred to have taken place in the late Archaean or early Proterozoic (2–2.5 Ga), enriched a depleted peridotite protolith resulting in extreme variations in Nd isotopic compositions (Long *et al.*, 1991). By contrast, the relatively young lithospheric mantle of the Midland Valley and Southern Uplands Terranes has much greater isotopic homogeneity.

Mantle xenoliths within the North Atlantic and Baffin Bay Palaeogene magmatic provinces appear to be restricted to very few localities and the only other location known in the British Isles is Inver, Co. Donegal (Kirstein & Timmerman, 2000). Spinel lherzolite xenoliths from a Palaeogene dyke in west Greenland (Larsen, 1982) appear to provide some parallels with the Loch Roag situation in that they contain alkali feldspar. In particular, they contain small amounts of phlogopite, hyalophane (Na_2O 5.65 wt%: K_2O 6.54 wt%: BaO 3.13 wt%) and chlorite, the latter within sieve-textured clinopyroxene, possibly pseudomorphing glass. Larsen (1982)

also refers to plagioclase (+ phlogopite) in another lherzolite xenolith: the plagioclase (not analysed) presumably being Na-rich**.**

The presence of feldspar in the Loch Roag samples could conceivably relate to a phase-change from spinel- to plagioclase-facies lherzolite, reflecting a reduction in pressure (*cf*. Rampone *et al*., 1993). Such a pressure release would be compatible with the Outer Hebrides lying close to the trailing edge of the sundered continental lithosphere where stretching and elevation of the SCLM would be anticipated. However a) the textural relationships differ markedly from those attending a facies change (Rampone *et al*., 1993) and b) the significant content of potassium would be inexplicable. Just as Larsen (1982) appealed to possible metasomatic introduction of material for the genesis of the phlogopite and hyalophane in the west Greenland case, so a metasomatic introduction of materials was the probable cause of the alkali feldspar - green clinopyroxene association in the Loch Roag xenoliths. Our REE data for the Loch Roag lherzolite clinopyroxenes amplify those of Menzies & Halliday (1988) and support the deduction by Long *et al*. (1991) that the geochemical and petrographic idiosyncrasies of the Loch Roag peridotites were due to percolation of a carbonatitic agent. The concurrence of both alkali addition (Na>K) and LREE enrichment suggests the possibility of metasomatism by natro-carbonatite melt as was noted in the case of data from Grande Comore xenoliths (Coltorti *et al*., 1999).

Furthermore these incompatible element enrichments (and associated isotopic singularities) cannot be considered unrelated to the megacryst suite that accompanies the peridotite and pyroxenite xenoliths. The megacryst suite has been shown (K-Ar and Ar-Ar dating; Menzies *et al*. (1988) and M. Timmerman, pers. comm.) to be very young (~47 Ma) whilst the isotopic signatures are an inheritance from ancient enrichment events (Long *et al*., 1991). The salic melts from which the megacryst

suite crystallised (Upton *et al*, 2009) may represent remobilised ancient and highly fusible metasomatic products that ascended in advance of the mafic (host) magma in the Palaeogene tectono-thermal event.

The pyroxenitic (*s.l.*) xenoliths are deduced to have arisen from a thick zone of ultramafic cumulates overlying tectonised peridotites. The former are regarded as constituting the base of the crust and the discontinuity between the two is considered analogous to the 'petrological Moho' of ophiolitic sequences. Gabbroic/dioritic meta-cumulates, broadly cogenetic to the pyroxenite cumulates, are inferred to overlie the latter, separated from them by a relatively sharp discontinuity (the 'seismic Moho'). The ultramafic and mafic cumulates represent complementary products of primitive basaltic magmas repetitively introduced along the density break coincident with the seismic Moho during magmatic episodes.

Acknowledgements

We gratefully acknowledge constructive criticisms of the manuscript made by E-R. Neumann, M. Grégoire and M. Coltorti. We also thank E-R Neumann for sharing her extensive dataset on mantle xenoliths and E. Handisyde for data on xenoliths from Fidra. Comments from an anonymous reviewer are also acknowledged. It is with great sadness that we report the death of our colleague P.G. Hill, prior to submission of this paper.

References

ALEXANDER, R.W.S., DAWSON, J.B., PATTERSON, E.M. & HERVIG, R.L. 1986. The megacryst and inclusion assemblage from the Black Rock vent, Ayrshire. *Scottish Journal of Geology*, **22**, 203-212.

582 ARAI, S. 1987. Japanese Island Arc: high alumina basalts, and calc-alkaline andesites
583 and dacites. In: NIXON P.H. (ed.) *Mantle Xenoliths*, Wiley, N.Y. 319-333.
584 ARAI, S., 1994. Characterisation of spinel peridotites by olivine-spinel compositional
585 relationship: a review and interpretation. *Chemical Geology*, **133**, 191-204.
586 ARTEMIEVA, I.M., THYBO, H. & KABAN, M.K. 2006. Deep Europe today: geophysical
587 synthesis of the upper mantle structure and lithospheric processes over 3.5 Ga.
588 In: GEE, D.G. & STEPHENSON, R.A.(eds.), *European Lithosphere*
589 *Dynamics*. *Geological Society of London Memoirs* **32**, 11-41.
590 ASENCIO, E., KNAPP, J.H., OWENS, T. J. & HELFFRICH, G. 2003. Mapping fine-scale
591 heterogeneities with the continental mantle lithosphere beneath Scotland:
592 Combining active and passive seismology. *Geology*, **31**, 477-480.
593 ASPEN, P., UPTON, B.G.J. & DICKIN, A.P. 1990. Anorthoclase, sanidine and associated
594 megacrysts in Scottish alkali basalts: high-pressure syenitic debris from upper
595 mantle sources? *European Journal of Mineralogy*, **2**, 503-517.
596 BAKER, M.B. & BECKETT, J.R. 1999. The origin of abyssal peridotites: a
597 reinterpretation of constraints based on primary bulk compositions. *Earth and*
598 *Planetary Science Letters* **171**, 49-61.
599 BAMFORD, D., NUNN, K., PRODEHL, C. & JACOB, B. 1977. LISPB-1V. Crustal
600 structure of northern Britain. *Geophysical Journal of the Royal Astronomical.*
601 *Society*, **54**, 43-60.
602 BASALTIC VOLCANISM STUDY PROJECT. 1981. Basaltic Magmatism on the Terrestrial
603 Planets. Pergamon Press Inc., New York, 1286 pp.
604 BODINIER, J-L., GARRIDO, C., CHANEFO, I., BRUGUIER, O. & GERVILLA, F. 2008.
605 Origin of pyroxenite-peridotite veined mantle by refertilisation reactions:

606 evidence from the Ronda peridotite (southern Spain) *Journal of Petrology*, **49**,
607 999-1025.
608 BONADIMAN, C., COLTORTI, M., DUGGEN, S., PALUDETTI, L., SIENA, F., THIRLWALL,
609 M.F. & UPTON, B.G.J. 2008. Palaeozoic subduction-related and
610 kimberlite/carbonatite metasomatism in the Scottish lithospheric mantle.
611 *Geological Society London, Special Publication.* **293**, 303-333.
612 COHEN R.S. O'NIONS, R.K., DAWSON, J.B. 1984. Isotope geochemistry of xenoliths
613 from East Africa: implications for development of mantle reservoirs and their
614 interaction. *Earth and Planetary Science Letters*, **68**, 209-220.
615 COLTORTI, M., BONADIMAN, C., HINTON, R.W., SIENA, F. & UPTON, B.G.J. 1999.
616 Carbonatite metasomatism of the oceanic upper mantle: evidence from
617 clinopyroxenes and glasses in ultramafic xenoliths of Grande Comore, Indian
618 Ocean. *Journal of Petrology*, **40**, 133-165.
619 COX, K.G. 1980. A model for flood basalt magmatism. *Journal of Petrology*, **21**, 629-
620 650.
621 DICK, H.J.B. & BULLEN, T. 1984. Chromian spinel as a petrogenetic indicator in
622 abyssal and alpine-type peridotites and spatially associated lavas.
623 *Contributions to Mineralogy and Petrology*, **86**, 54-56.
624 DOWNES, H. 1993. The nature of the lower continental crust in Europe: petrological
625 and geochemical evidence from xenoliths. *Physics of the Earth and Planet*
626 *Interiors*, **79**, 195-218.
627 DOWNES, H. 2001. Formation and Modification of the Shallow Sub-continental
628 Lithospheric Mantle: a Review of Geochemical Evidence from Ultramafic
629 Xenolith Suites and Tectonically Emplaced Ultramafic Massifs of Western
630 and Central Europe. *Journal of Petrology*, **42**, 233-250.

631 DOWNES, H. 2007. Origin and significance of spinel and garnet pyroxenites in the
632 shallow lithospheric mantle. *Lithos,* **99**, 1-24.
633 DOWNES, H., UPTON, B.G.J., HANDISYDE, E. & THIRLWALL, M.F. 2001. Geochemistry
634 of mafic and ultramafic xenoliths from Fidra (Southern Uplands, Scotland):
635 implications for lithospheric processes in Permo-Carboniferous times. *Lithos*,
636 **58**, 105-124.
637 DOWNES, H., UPTON, B.G.J., CONNOLLY, J., BEARD, A.D. & BODINIER, J-L. 2007.
638 Petrology and geochemistry of a cumulate xenolith suite from Bute: evidence
639 for late Palaeozoic crustal underplating beneath SW Scotland. *Journal of the*
640 *Geology Society of London*, **164**, 1-15.
641 DRUMMOND, B.J. & COLLINS, C.D.N. 1986. Seismic evidence for underplating of the
642 lower continental crust. *Earth and Planetary Science Letters*, **79**, 361-372.
643 FAITHFULL, J. & UPTON, B.G.J. 2006. Xenolithic insights into the deep geology
644 beneath the Ross of Mull. *Scottish Journal of Geology*, **42**, 37-41.
645 FREY, F.A. & PRINZ, M. 1978. Ultramafic inclusions from San Carlos, Arizona:
646 petrologic and geochemical data bearing on their petrogenesis. *Earth and*
647 *Planetary Science Letters*, ***38***, 129-176.
648 GEE, D.G. & STEPHENSON, R. A., 2006. The European lithosphere: an introduction.
649 In: GEE D.G. & STEPHENSON, R.A. (eds.) *European Lithosphere*
650 *Dynamics. Geological Society of London, Memoirs*, **32**, 313-322.
651 GOTO, K. & ARAI, S. 1987. Petrology of peridotite xenoliths in lamprophyre from
652 Shingu, southwestern Japan: implications for origin of Fe-rich peridotites.
653 *Mineralogy and Petrology*, **37**, 137-155.
654 GREENBAUM, D. 1972. Magmatic processes at ocean ridges: evidence from the
655 Troodos Massif, Cyprus. *Nature Physical Sciences*, **238**, 18-21.

656 GRIFFIN, W.L. & O'REILLY, S.Y. 1987a. Is the continental Moho the crust-mantle
657 boundary? *Geology*, **15**, 241-244.
658 GRIFFIN, W.L. & O'REILLY, S.Y. 1987b. The composition of the lower crust and the
659 nature of the continental Moho – xenolith evidence. In: NIXON, P.H.(ed.),
660 *Mantle Xenoliths*, 413-430. John Wiley & Sons Ltd., New York.
661 GRIFFIN, W.L., O'REILLY, S.Y., AFONSO, J.C. & BEGG, G.C. 2009. The Composition
662 and Evolution of Lithospheric Mantle: a Re-evaluation and its Tectonic
663 Implications. *Journal of Petrology*, **50**, 1185-1204.
664 HALLIDAY, A. N., DICKIN, A.P., HUNTER, R.H., DAVIES, G.R., DEMPSTER, T.J.,
665 HAMILTON, P.J. & UPTON, B.G.J. 1993. Formation and composition of lower
666 continental crust: evidence from Scottish xenolith suites. *Journal of*
667 *Geophysical Research*, **98**, 581-607.
668 HUNTER, R.H. & UPTON, B.G.J. 1987. The British Isles – a Palaeozoic mantle sample.
669 In: NIXON P.H. (ed.), *Mantle Xenoliths*, 107-118. John Wiley & Sons Ltd.,
670 New York.
671 IRVING, A.J., 1980. Petrology and geochemistry of composite ultramafic xenoliths in
672 alkali basalts and implications for magmatic processes within the mantle.
673 *American Journal of Science*, **280-A**, 389-426.
674 JOHNSON, K.T.M. DICK, H.J.B & SHIMIZU, N. 1990. Melting in the oceanic upper
675 mantle: an ion microprobe study of diopsides in abyssal peridotites. *Journal of*
676 *Geophysical Research*, **97**, 9219-9242.
677 KIRSTEIN L.A. & TIMMERMAN, M.J., 2000. Evidence of the proto-Iceland plume in
678 northwestern Ireland at 42Ma from helium isotopes. *Journal of the Geological*
679 *Society London*, **157**, 923-927.

KIRSTEIN L.A., DUNAI, T., DAVIES, G., UPTON, B.J., 2004. Evidence of heterogenous mantle beneath Scotland during the Permo-Carboniferous from helium isotopes. In: WILSON, M., NEUMANN, E-R., DAVIES, G-R., TIMMERMANN, M.J., HEEREMANS, M., LARSEN, B.T. (eds), Permo-Carboniferous magmatism and rifting in Europe, *Geological Society of London, Special Publication* **223**, 243-258.

KIRSTEIN L.A, DAVIES, G.R., HEEREMANS, M. 2006. The petrogenesis of Carboniferous-Permian dyke and sill intrusions across northern Europe. *Contributions to Mineralogy and Petrology,* **152**, 721-742.

LARSEN, J.G. 1982. Mantle derived dunite and lherzolite nodules from Ubekendt Ejland, west Greenland Tertiary Province. *Mineralogical Magazine*, **46**, 329-336.

LIPPARD, S.J., SHELTON, A.W. & GASS, I.G. 1986. The ophiolite of Northern Oman. Memoir No. 11, Geological Society, London. Blackwell Scientific Publications, Oxford. 178 pp.

LONG, A.M., MENZIES, M.A., THIRLWALL, M.F., UPTON, B.G.J. & ASPEN, P. 1991. Carbonatite – mantle interaction: a possible origin for megacryst/xenolith suites in Scotland. In: MEYER, H.O.A. & LEONARDOS, O.H. (eds.). *Kimberlites, Related Rocks and Mantle Xenoliths*. 5th International Kimberlite Conference, Brazil, **1**, 467-477. Comp. Pasquisa Recursos Minerais, Brazil.

LLOYD, F.E. 1981. Upper mantle metasomatism beneath a continental rift: clinopyroxenes in alkali mafic lavas and nodules from south-west Uganda. *Mineralogical Magazine*, **44**, 315-323.

MACDONALD, R. & FETTES, D.J., 2007. The tectonomagmatic evolution of Scotland. *Transactions of the Royal Society of Edinburgh, Earth Sciences*, **97**, 213-295.

MCDONOUGH W.F. & SUN, S-S. 1995. The composition of the Earth, *Chemical Geology*, **120**, 223-253.

MCDONOUGH W.F. & RUDNICK, R.K. 1998. Mineralogy and composition of the upper mantle. In: HEMLEY, R.J., (ed.) Ultrahigh-Pressure Mineralogy: Physics and Chemistry of the Earth's Deep Interior. *Mineralogical Society of America, Reviews in Mineralogy,* **37**, 139 - 164.

MEEN, J.K. 1987. Mantle metasomatism and carbonatites: an experimental study of a complex relationship. *Geological Society of America, Special Paper*, **215**, 91-100.

MENZIES, M. A. & HALLIDAY, A. N. 1984a. Isotopic evidence for mantle heterogeneity beneath the Midland Valley and adjacent regions from studies of inclusion suites. *Transactions Royal Society Edinburgh Earth Science*, **75**, 298-299.

MENZIES, M. A. & HALLIDAY, A. N. 1984b. Enriched mantle below the Scottish Highlands: Sr and Nd isotope and rare earth elements in peridotite and pyroxenite xenoliths from Loch Roag, Streap Comlaidh and Kilchatten, Scotland. Abstract, v. **V**. (Sects. 10.11) p 348, 27th International Geological Congress. (Moscow).

MENZIES, M. & HALLIDAY, A. 1988. Lithospheric mantle domains beneath the Archean and Proterozoic crust of Scotland. *Journal of Petrology*, *Special Lithosphere Issue*, 275-302.

MENZIES, M.A., HALLIDAY, A.N., PALACZ, Z., HUNTER, R.H., ASPEN, P. & HAWKESWORTH, C.J. 1987. Evidence from mantle xenoliths for an enriched keel under the Outer Hebrides. *Nature*, **325**, 44-47.

729 MENZIES, M.A., HALLIDAY, A.N., HUNTER, R.H., MACINTYRE, R.M. & UPTON, B.G.J.
730 1988. The age, composition and significance of a xenolith-bearing
731 monchiquite dike, Lewis, Scotland. In: ROSS, J, JAQUES, A.L, FERGUSON, J.,
732 GREEN, D.H., O'REILLY, S.Y., DANCHIN, D.Y. & JANSE, A.J.A. (eds.).
733 Kimberlites and Related Rocks **2**. Their mantle/crust setting, diamonds and
734 diamond exploration. *Geological Society of Australia Special Publication* No.
735 **14**, 843-852, Blackwell Scientific Publications.

736 RAMPONE, E., PICCARDO, G.B., VANUCCI, R., BOTAZZI, P. & OTTOLINI, L. 1993.
737 Subsolidus reactions monitored by trace element partitioning: the spinel- to
738 plagioclase-facies transition in mantle peridotites. *Contributions to*
739 *Mineralogy and Petrology*, **115**, 1-17

740 RINGWOOD., A.E. 1975. Composition and petrology of the Earth's Mantle. 618 pp.
741 McGraw-Hill, New York.

742 ROGERS, N.W. 1977. Granulite xenoliths from Lesotho kimberlites and the lower
743 continental crust. *Nature*, London, **270**, 681-684.

744 RUDNICK, R.L. 1992. Restites, Eu anomalies, and the lower continental crust.
745 *Geochimica et Cosmochimica Acta*, **56**, 963-970.

746 SCHIANO, P, & CLOCCHIATTI, R., 1994. Worldwide occurrences of silica-rich sub-
747 continental and sub-oceanic mantle minerals. *Nature*, **368**, 621-624.

748 SINGH, C. & MCKENZIE, D. 1993. Layering in the lower crust, *Geophysical Journal*
749 *International*, **113**, 622-628.

750 SIMON, N.S.C., NEUMANN, E-R, BONADIMAN, C., COLTORTI, M., DELPECH, G.,
751 GRÈGOIRE, M. & WIDOM, E. 2008. Ultra-refractory domains in the oceanic
752 mantle lithosphere sampled as mantle xenoliths at ocean islands. *Journal of*
753 *Petrology*, **49**, 1223-1251.

754 SMEDLEY, P.L., 1988. Trace element and isotope variations in Scottish and Irish
755 Dinantian volcanism: evidence for an OIB-like mantle source. *Journal of*
756 *Petrology*, **29**, 413-443.
757 UPTON, B.G.J., ASPEN, P. & CHAPMAN, N.A. 1983. The upper mantle and deep crust
758 beneath the British Isles: evidence from inclusions in volcanic rocks. *Journal*
759 *of the Geological Society of London*, **140**, 105-121.
760 UPTON, B.G.J., ASPEN, P., REX., D.C., MELCHER, F. & KINNY, P. 1998. Lower crustal
761 and possible shallow mantle samples from beneath the Hebrides: evidence
762 from a xenolithic dyke at Gribun, western Mull. *Journal of the Geological*
763 *Society of London*, **155**, 813-828.
764 UPTON, B.G.J., ASPEN, P. & HINTON, R.W. 2001. Pyroxenite and granulite xenoliths
765 from beneath the Scottish Northern Highlands Terrane: evidence for lower-
766 crust/upper-mantle relationships. *Contributions to Mineralogy and Petrology*,
767 **142**, 178-197.
768 UPTON, B.G.J., ASPEN, P. & HINTON, R.W. 2003. Garnet pyroxenite xenoliths and
769 pyrope megacrysts in Scottish alkali basalts. *Scottish Journal of Geology*, **39**,
770 169-184.
771 UPTON, B.G.J., HINTON, R.W., ASPEN, P., FINCH. A. & VALLEY, J.W. 1999.
772 Megacrysts and associated xenoliths: evidence for migration of geochemically
773 enriched melts in the upper mantle beneath Scotland. *Journal of Petrology*, **40**,
774 935-956.
775 UPTON, B.G.J., STEPHENSON, D., SMEDLEY, P.M., WALLIS, S.M. & FITTON, J.G. 2004.
776 Carboniferous and Permian magmatism in Scotland. In: WILSON, M.,
777 NEUMANN, E.R., DAVIES, G.R., TIMMERMAN, M.J., HEEREMANS, M. &
778 LARSEN, B.T. (eds.) Permo-Carboniferous Magmatism and Rifting in Europe.

Geological Society of London Special Publication, **223**, 195-218. The Geological Society, London.

UPTON, B.G.J., FINCH, A.A. & SLABY, E. 2009. Megacrysts and salic xenoliths in Scottish alkali basalts: derivatives of deep crustal intrusions and small-melt fractions from the upper mantle. *Mineralogical Magazine*, **73**, 943-956.

WALLIS, S.M. 1989. Petrology and geochemistry of Upper Carboniferous – Lower Permian Volcanic Rocks in Scotland. *Unpublished Ph.D. thesis*, Edinburgh University.

WHITE, R.W. 1966. Ultramafic inclusions in basaltic rocks from Hawaii. *Contributions to Mineralogy and Petrology*, **12**, 245-314.

WILSHIRE, H.G. & PIKE, J.E.N. 1975. Upper mantle diapirism: evidence from analogous features in alpine peridotite and ultramafic inclusions in basalt. *Geology*, **3**, 467-470.

WILSHIRE H.G., & SHERVAIS, J.W. 1975. Al-augite and Cr-diopside in ultramafic xenoliths from the western United States. *Physical Chemistry of the Earth*, **9**, 257-272.

WOODCOCK, N.H. & STRACHAN, R.A. (eds) 2000. Geological History of Britain and Ireland. Oxford, Blackwell Science.

WORKMAN, R.K & HART, R.H 2005. Major and trace element composition of the depleted MORB mantle (DMM). *Earth and Planetary Science Letters,* **231**, 53-72.

Figure captions

Fig. 1. Map showing the principal tectonic terranes and xenolith localities across Scotland. LR, Loch Roag: RNB, Rinibar: DCN, Duncansby Ness: STP, Streap Com'Laidh: RSK, Riska: GRB, Gribun: FNP, Fionnphort: KTN, Kilchatten: ISL, Islay: HN, Hawks Nib: MCR, Machrihanish: BR, Black Rocks: RP, Ruddon's Point: EN, Elie Ness: FD, Fidra: Old, Oldhamstocks: HEX, Hexpath: CF, Cooms Fell.

Fig. 2. MgO vs. NiO wt% plotted for olivines from spinel lherzolite xenoliths from Scotland.

Fig. 3. Cr# spinel vs. Mg# olivines from Scottish lherzolite xenoliths showing the olivine-spinel mantle array (Arai, 1994).

Fig. 4. Cr# vs. Mg# for spinels from the Scottish lherzolite xenoliths.

Fig. 5. CaO vs. Al_2O_3 wt% for clinopyroxenes. **A:** data for Scottish xenolith localities. **B:** comparative fields for spinel lherzolite xenoliths from other continental provinces worldwide.

Fig. 6. MgO vs. Al_2O_3 wt% plot for orthopyroxenes from the Scottish lherzolite xenoliths. PM_{opx} (large open square) is based on mass balance calculations using major element composition and modal proportions (spinel stability field) for PUM from McDonough & Sun (1995). The theoretical residual trend is calculated using equations from Workman & Hart (2005). The trend is interrupted at the calculated melting percentage for complete pyroxene consumption (opx 30%; cpx 25%).

Fig.7. MgO vs. Al_2O_3 wt% for clinopyroxenes from Scottish lherzolite xenoliths. The theoretical residual trend is calculated using the equations from Workman & Hart (2005).

827 Fig. 8. $^{143}Nd/^{144}Nd$ vs. $^{87}Sr/^{86}Sr$ for whole-rocks and clinopyroxenes from Scottish
828 lherzolite xenoliths. Selected data from Menzies & Halliday, 1988; Downes et al.,
829 2001; 2007; Bonadiman et al., 2008.
830 Fig. 9. Chondrite-normalised REE patterns for clinopyroxene in Scottish peridotite
831 xenoliths. C1 chondrite normalization values of McDonough & Sun (1995).

Table 1b. Selected spinel analyses for key xenolith localities.

	C Fell C	CnB 51	RNB 5	Hex 1	HN 31	RP 77	Rsk 1	STP1	Fid-1	Fid-2	LR80-1	LR80-2	LR81-1	LR81-2
SiO_2	0.05	0.03	0.06	0.05	0.08	0.05	0.03	0.05	0.04	0.07	0.02	0.02	0.01	0.05
TiO_2	0.06	0.05	0.06	0.05	0.06	0.08	0.18	0.12	0.20	0.66	0.33	0.53	0.23	0.51
Al_2O_3	55.23	59.74	25.79	49.98	60.57	57.98	40.40	52.99	54.93	55.82	31.87	16.25	36.41	19.45
Cr_2O_3	10.89	7.80	39.63	16.29	6.17	9.06	27.00	15.44	9.27	9.91	34.58	49.46	30.31	46.18
Fe_2O_3	3.45	1.53	5.78	3.75	3.03	2.34	3.14	1.31	4.59	1.57	4.48	6.03	4.15	5.77
FeO	7.43	9.38	12.17	9.94	7.59	8.55	10.87	9.19	13.61	10.20	13.53	14.14	12.91	14.03
MnO	0.12	0.13	0.23	0.18	0.10	0.12	0.21	0.11	0.24	0.08	0.16	0.19	0.13	0.17
NiO	0.39	0.40	0.00	0.36	0.31	0.42	0.26	0.35	0.29	0.36	0.17	0.16	0.22	0.14
MgO	21.12	20.52	15.21	19.15	21.86	20.80	17.55	20.02	17.51	19.90	15.21	13.08	16.11	13.49
CaO	0.03	0.01	n.d	0.01	0.00	0.01	0.01	0.00	0.00	0.02	<0.02	<0.02	<0.02	<0.02
Na_2O	0.01	0.01	n.d	0.01	0.01	0.03	0.02	n.d	n.d	n.d	n.d.	n.d.	n.d.	n.d.
K_2O	0.01	0.01	n.d	0.01	0.00	0.01	0.01	n.d	n.d	n.d	n.d.	n.d.	n.d.	n.d.
Total	**98.79**	**99.59**	**98.93**	**99.77**	**99.79**	**99.45**	**99.66**	**99.58**	**100.68**	**98.59**	**100.35**	**99.86**	**100.48**	**99.79**
	Formulae based on 32 Oxygens & 16 Tetrahedral Cations													
Si^{4+}	0.010	0.005	0.015	0.012	0.016	0.010	0.007	0.010	0.009	0.015	0.005	0.006	0.001	0.011
Ti^{4+}	0.009	0.008	0.011	0.008	0.010	0.012	0.029	0.019	0.032	0.105	0.058	0.101	0.04	0.095
Al^{3+}	13.633	14.482	7.349	12.616	14.519	14.132	10.657	13.197	13.680	13.902	8.768	4.846	9.784	5.713
Cr^{3+}	1.804	1.268	7.575	2.759	0.992	1.481	4.777	2.578	1.549	1.654	6.381	9.897	5.464	9.099
Fe^{3+}	0.544	0.237	1.052	0.604	0.464	0.364	0.529	0.208	0.730	0.250	0.787	1.149	0.712	1.081
Fe^{2+}	1.301	1.612	2.460	1.780	1.292	1.479	2.035	1.624	2.405	1.802	2.641	2.992	2.461	2.925
Mn^{2+}	0.022	0.022	0.047	0.032	0.018	0.021	0.040	0.020	0.044	0.014	0.032	0.04	0.026	0.035
Ni^{2+}	0.066	0.066	0.000	0.062	0.051	0.070	0.046	0.057	0.048	0.060	0.033	0.032	0.04	0.028
Mg^{2+}	6.592	6.289	5.480	6.112	6.624	6.411	5.855	6.304	5.512	6.264	5.295	4.935	5.474	5.011
Ca^{2+}	0.007	0.002	0.000	0.002	0.001	0.002	0.001	0.000	0.000	0.005	0.000	0.000	0.000	0.000
Na^{+}	0.002	0.004	0.000	0.003	0.004	0.012	0.007	0.000	0.000	0.000	0.000	0.000	0.000	0.000
K^{+}	0.002	0.001	0.000	0.002	0.001	0.002	0.002	0.000	0.000	0.000	0.000	0.000	0.000	0.000
ΣCations	**24**	**24**	**24**	**24**	**24**	**24**	**24**	**24**	**24**	**24**	**24**	**24**	**24**	**24**
	Calculated Site Occupancy													
$Total_{iv}$	16	16	16	16	16	16	16	16	16	16	16	16	16	16
$Total_{vi}$	8	8	8	8	8	8	8	8	8	8	8	8	8	8
Σ Cations	24	24	24	24	24	24	24	24	24	24	24	24	24	24
Cr#	11.68	8.05	50.76	17.94	6.39	9.49	30.95	16.34	10.17	10.63	42.12	67.13	35.83	61.43

Selected Analyses of Minerals in Scottish Peridotites

Table 2. Selected orthopyroxene analyses.

	C Fell C	CnB 51	RNB 5	Hex 1	HN 31	RP 77	Rsk 1	STP5	STP1	FD124	FD127	LR80	LR81
SiO_2	52.91	55.31	56.20	54.16	54.59	54.64	55.90	55.23	55.96	54.76	54.30	57.06	56.66
TiO_2	0.18	0.10	0.02	0.09	0.06	0.08	0.07	0.14	0.11	0.16	0.00	0.09	0.09
Al_2O_3	5.38	3.74	2.01	4.08	5.11	4.30	2.27	4.41	3.85	4.30	4.37	2.16	2.65
Cr_2O_3	0.63	0.25	0.29	0.41	0.21	0.31	0.37	0.35	0.40	0.41	0.29	0.42	0.38
FeO	5.14	6.66	6.18	7.65	6.06	6.45	5.55	5.35	6.05	6.90	8.39	6.34	6.56
MnO	0.13	0.17	0.20	0.19	0.14	0.16	0.14	0.15	0.14	0.14	0.23	0.18	0.18
NiO	0.10	0.09	n.d	0.11	0.07	0.10	0.09	0.00	0.13	n.d	n.d	0.06	0.08
MgO	27.22	33.34	33.93	32.54	32.86	32.99	34.69	33.09	32.61	32.11	31.24	33.77	33.62
CaO	7.49	0.34	0.81	0.70	0.95	0.68	0.37	0.79	0.58	0.75	0.82	0.45	0.48
Na_2O	0.55	0.08	0.12	0.11	0.08	0.14	0.04	0.13	0.11	0.27	0.39	0.10	0.09
K_2O	0.01	0.00	0.02	0.01	0.00	0.01	0.01	0.01	n.d.	n.d.	n.d.	n.d.	n.d.
Total	**99.73**	**100.07**	**99.78**	**100.06**	**100.13**	**99.86**	**99.50**	**99.65**	**99.93**	**99.81**	**100.03**	**100.60**	**100.76**
Formula based on 6 Oxygens													
Si^{4+}	1.868	1.912	1.947	1.887	1.884	1.895	1.935	1.907	1.930	1.903	1.898	1.959	1.943
Ti^{4+}	0.005	0.003	0.001	0.002	0.002	0.002	0.002	0.004	0.003	0.004	0.000	0.002	0.002
Al^{3+}	0.224	0.152	0.082	0.168	0.208	0.176	0.093	0.179	0.156	0.176	0.180	0.088	0.107
Cr^{3+}	0.018	0.007	0.008	0.011	0.006	0.009	0.010	0.010	0.011	0.011	0.008	0.012	0.010
Fe^{2+}	0.152	0.193	0.179	0.223	0.175	0.187	0.161	0.154	0.174	0.201	0.245	0.182	0.188
Mn^{2+}	0.004	0.005	0.006	0.006	0.004	0.005	0.004	0.004	0.004	0.004	0.007	0.006	0.005
Ni^{2+}	0.003	0.002	0.000	0.003	0.002	0.003	0.003	0.000	0.004	0.000	0.000	0.002	0.002
Mg^{2+}	1.432	1.718	1.751	1.690	1.690	1.705	1.789	1.703	1.677	1.663	1.627	1.729	1.719
Ca^{2+}	0.283	0.013	0.030	0.026	0.035	0.025	0.014	0.029	0.021	0.028	0.031	0.017	0.018
Na^{+}	0.037	0.005	0.008	0.008	0.005	0.010	0.003	0.009	0.007	0.018	0.026	0.006	0.006
K^{+}	0.000	0.000	0.001	0.000	0.000	0.000	0.001	0.000	0.000	0.000	0.000	0.000	0.000
ΣCations	**4**	**4**	**4**	**4**	**4**	**4**	**4**	**4**	**4**	**4**	**4**	**4**	**4**
End-Members													
En	**76.5**	**89.1**	**89.1**	**86.9**	**88.8**	**88.7**	**90.9**	**90.1**	**89.6**	**87.9**	**85.5**	**89.4**	**89.1**
Fs	**8.3**	**10.2**	**9.4**	**11.8**	**9.4**	**10.0**	**8.4**	**8.4**	**9.3**	**10.6**	**12.9**	**9.7**	**10.0**
Wo	**15.1**	**0.7**	**1.5**	**1.3**	**1.8**	**1.3**	**0.7**	**1.5**	**1.1**	**1.5**	**1.6**	**0.9**	**0.9**

Selected Analyses of Minerals in Scottish Peridotites

				Table 2 cont. Selected clinopyroxene analyses.												
	C Fell C	**CnB 51**	**RNB 5**	**Hex 1**	**HN 31**	**RP 77**	**RP289**	**Rsk 1**	**STP5**	**FD124**	**FD127**	**LR80**	**LR81**			
SiO_2	51.35	52.08	52.44	51.58	51.36	51.84	51.36	52.02	52.36	52.14	52.01	54.55	53.78			
TiO_2	0.38	0.70	0.20	0.28	0.30	0.50	0.76	0.31	0.58	0.67	0.72	0.34	0.42			
Al_2O_3	6.03	6.22	3.92	5.79	6.47	6.87	5.35	3.41	6.71	6.92	7.02	4.22	4.71			
Cr_2O_3	0.86	0.56	1.31	0.87	0.34	0.68	1.30	1.07	0.71	0.74	0.72	1.09	0.86			
FeO	2.62	2.37	2.96	3.76	3.25	2.83	4.65	1.94	2.61	3.08	3.46	3.10	3.08			
MnO	0.09	0.08	0.11	0.12	0.09	0.10	0.19	0.08	0.09	0.00	0.08	0.08	0.08			
NiO	0.05	0.05	n.d	0.06	0.05	0.06	0.04	0.05	0.00	0.00	0.18	0.02	0.04			
MgO	15.49	14.57	16.58	15.46	16.47	15.02	15.80	16.40	15.44	15.21	15.32	14.69	14.63			
CaO	21.36	20.98	21.00	20.09	20.69	19.98	19.75	23.11	19.65	20.38	19.75	19.80	20.45			
Na_2O	1.43	1.98	1.06	1.59	0.96	1.93	0.90	0.77	1.84	1.54	1.33	2.56	2.32			
K_2O	0.00	0.01	0.01	0.00	0.01	0.01	n.d.	0.01	0.01	n.d.	n.d.	n.d.	n.d.			
Total	**99.65**	**99.59**	**99.59**	**99.60**	**99.99**	**99.82**	**100.09**	**99.16**	**100.00**	**100.67**	**100.43**	**100.45**	**100.37**			
Formula based on 6 Oxygens																
Si^{4+}	1.872	1.893	1.913	1.884	1.862	1.879	1.873	1.909	1.888	1.874	1.871	1.959	1.934			
Ti^{4+}	0.010	0.019	0.005	0.008	0.008	0.014	0.021	0.009	0.016	0.018	0.019	0.009	0.011			
Al^{3+}	0.259	0.266	0.169	0.249	0.276	0.294	0.230	0.148	0.285	0.293	0.298	0.178	0.200			
Cr^{3+}	0.025	0.016	0.038	0.025	0.010	0.020	0.037	0.031	0.020	0.021	0.020	0.031	0.024			
Fe^{2+}	0.080	0.072	0.090	0.115	0.099	0.086	0.142	0.059	0.079	0.093	0.104	0.093	0.093			
Mn^{2+}	0.003	0.002	0.003	0.004	0.003	0.003	0.006	0.002	0.003	0.000	0.002	0.002	0.002			
Ni^{2+}	0.001	0.002	0.000	0.002	0.002	0.002	0.001	0.001	0.000	0.000	0.005	0.001	0.001			
Mg^{2+}	0.841	0.789	0.901	0.842	0.890	0.811	0.859	0.897	0.830	0.815	0.821	0.786	0.784			
Ca^{2+}	0.834	0.817	0.821	0.786	0.804	0.776	0.772	0.909	0.759	0.785	0.761	0.762	0.788			
Na^{+}	0.101	0.140	0.075	0.113	0.067	0.136	0.064	0.055	0.129	0.107	0.093	0.178	0.162			
K^{+}	0.000	0.001	0.000	0.000	0.000	0.000	0.000	0.000	0.000	0.000	0.000	0.000	0.000			
ΣCations	**4**	**4**	**4**	**4**	**4**	**4**	**4**	**4**	**4**	**4**	**4**	**4**	**4**			
End-Members																
En	**47.8**	**47.0**	**49.6**	**48.2**	**49.6**	**48.4**	**48.5**	**48.0**	**49.7**	**48.1**	**48.7**	**47.9**	**47.1**			
Fs	**4.7**	**4.4**	**5.2**	**6.8**	**5.6**	**5.3**	**8.0**	**3.3**	**4.9**	**5.5**	**6.2**	**5.7**	**5.6**			
Wo	**47.4**	**48.6**	**45.2**	**45.0**	**44.8**	**46.3**	**43.5**	**48.7**	**45.5**	**46.4**	**45.1**	**46.6**	**47.3**			

Table 3. Feldspar analyses.

	LR80	LR81
SiO_2	65.87	65.86
TiO_2	0.03	0.04
Al_2O_3	21.20	21.46
Cr_2O_3	0.00	0.00
FeO	0.16	0.23
MnO	0.00	0.00
NiO	0.00	0.00
MgO	0.09	0.04
CaO	2.25	2.39
Na_2O	9.38	9.64
K_2O	1.33	0.94
Total	**100.31**	**100.60**
Formula based on 32 Oxygens		
Si^{4+}	11.613	11.566
Ti^{4+}	0.004	0.005
Al^{3+}	4.405	4.442
Cr^{3+}	0.000	0.000
Fe^{2+}	0.024	0.034
Mn^{2+}	0.000	0.000
Ni^{2+}	0.000	0.000
Mg^{2+}	0.024	0.010
Ca^{2+}	0.425	0.450
Na^{+}	3.206	3.282
K^{+}	0.299	0.211
ΣCations	**20**	**20**
End-Members		
Ab	**81.6**	**83.3**
An	**10.8**	**11.4**
Or	**7.6**	**5.3**

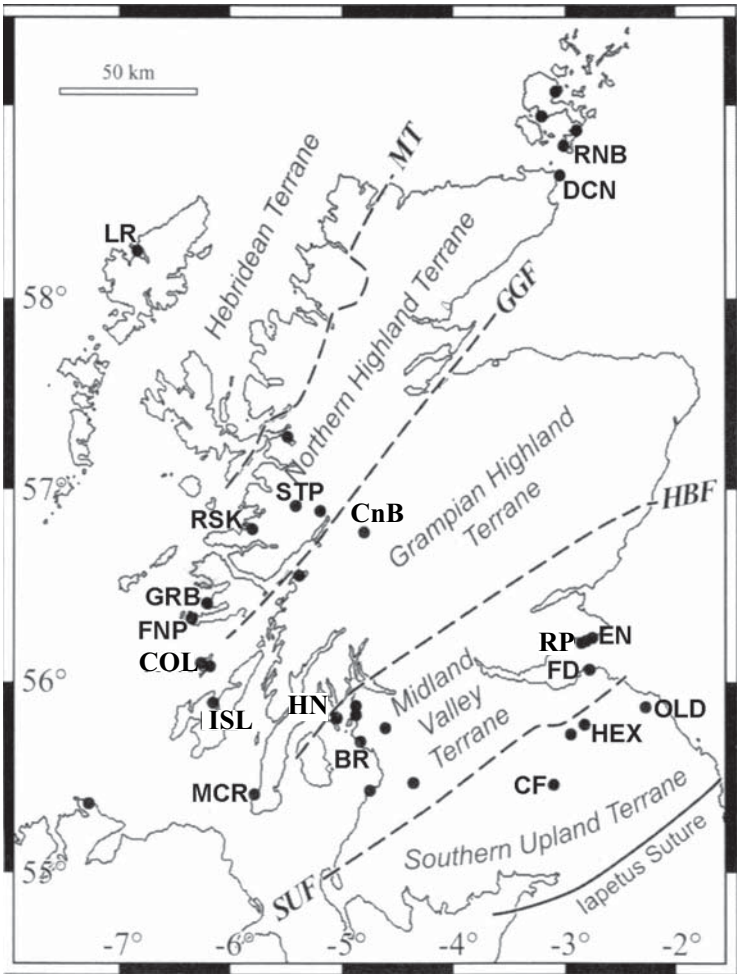
50 km
RNB
DCN
LR
MT
Hebridean Terrane
Northern Highland Terrane
GGF
58°
57°
STP
RSK
CnB
Grampian Highland Terrane
HBF
GRB
FNP
COL
RP
EN
FD
56°
HN
ISL
Midland Valley Terrane
OLD
HEX
BR
CF
MCR
Southern Upland Terrane
SUF
Iapetus Suture
55°
-7°
-6°
-5°
-4°
-3°
-2°

Figure 1.

Figure 2.

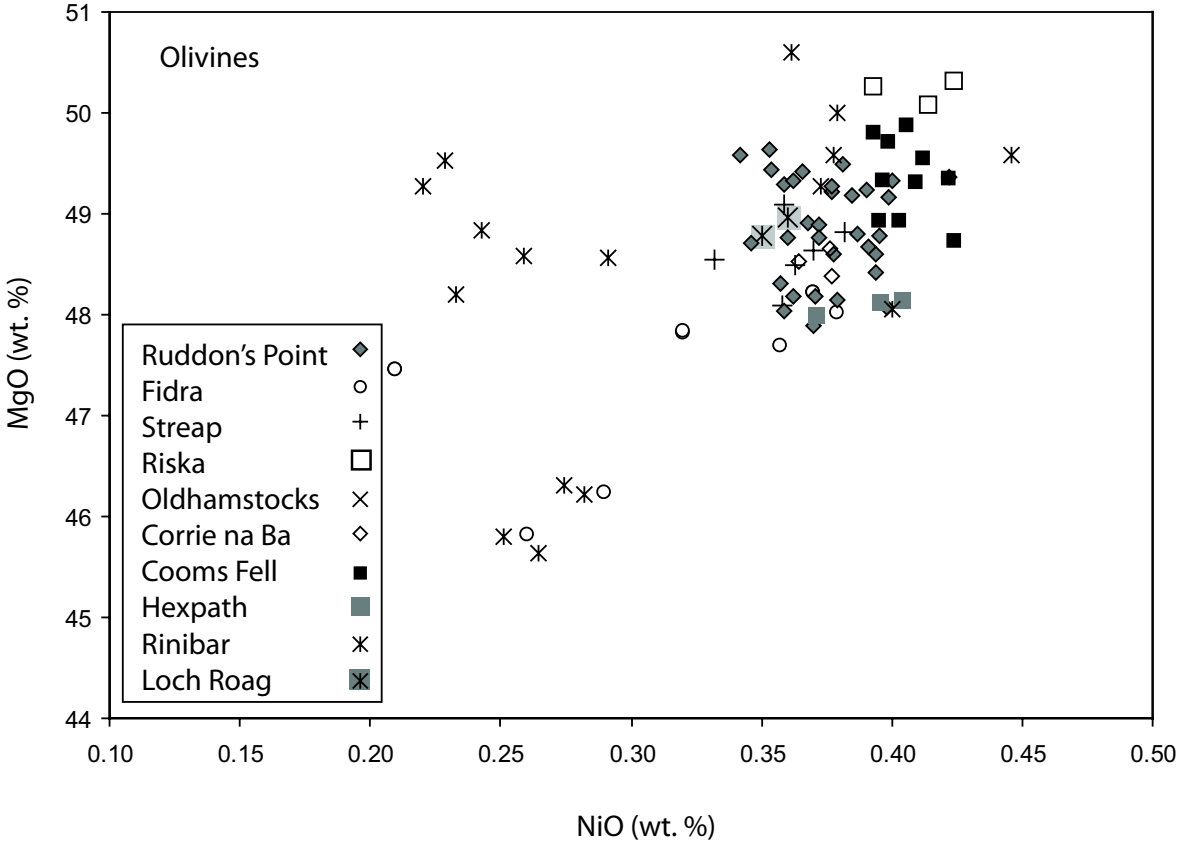
Olivines
MgO (wt. %)
NiO (wt. %)
51
50
49
48
47
46
45
44
0.10
0.15
0.20
0.25
0.30
0.35
0.40
0.45
0.50
Ruddon's Point
Fidra
Streap
Riska
Oldhamstocks
Corrie na Ba
Cooms Fell
Hexpath
Rinibar
Loch Roag

Figure 3.

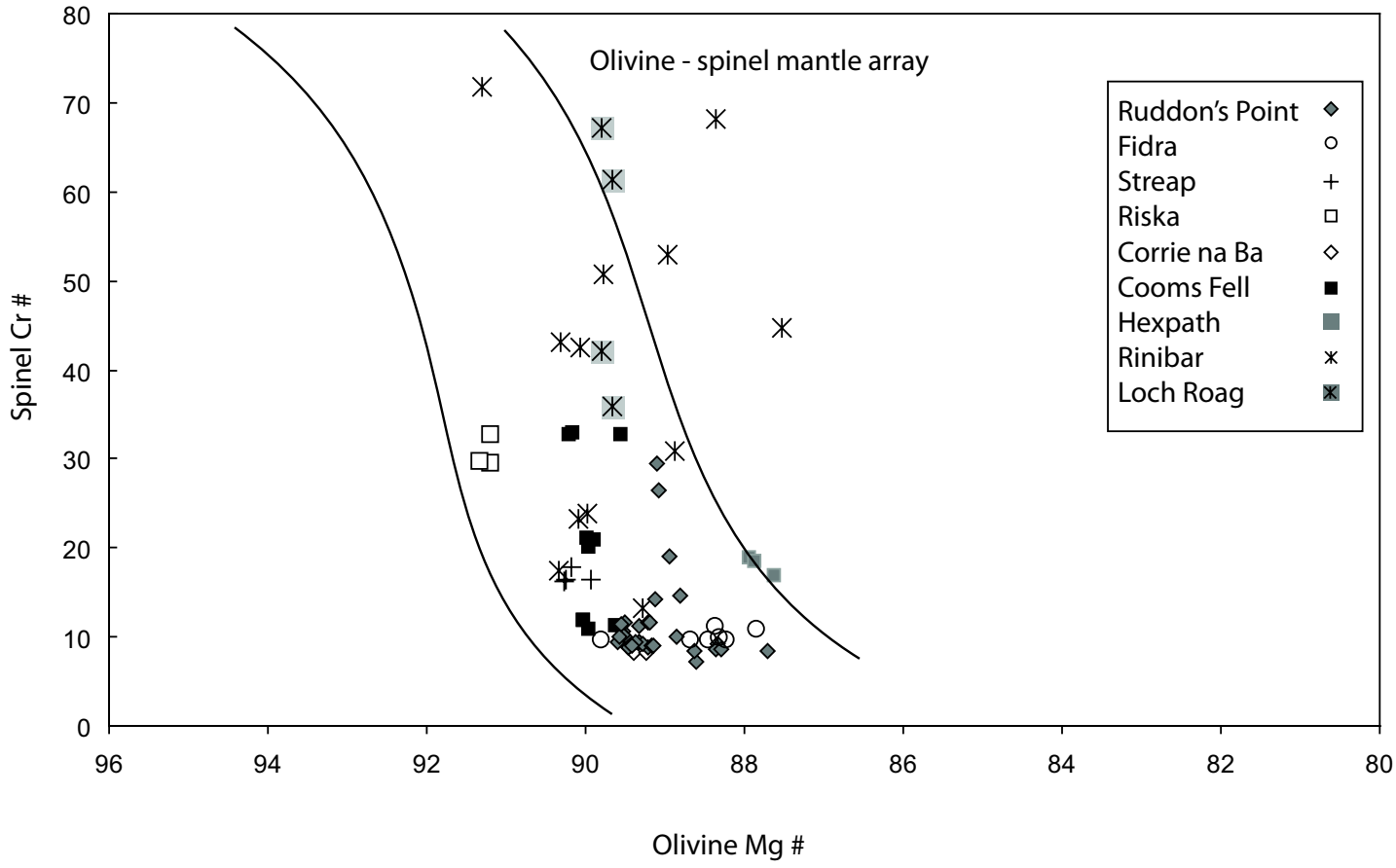
Olivine - spinel mantle array
Ruddon's Point
Fidra
Streap
Riska
Corrie na Ba
Cooms Fell
Hexpath
Rinibar
Loch Roag
Spinel Cr #
Olivine Mg #
80
70
60
50
40
30
20
10
0
96
94
92
90
88
86
84
82
80

Figure 4.

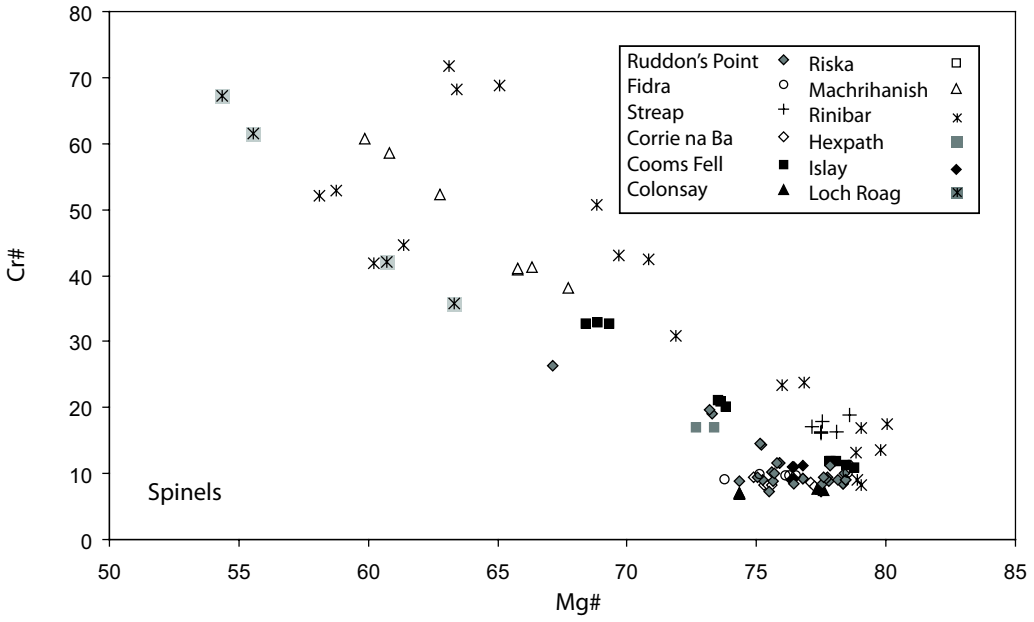
Ruddon's Point
Fidra
Streap
Corrie na Ba
Cooms Fell
Colonsay
Riska
Machrihanish
Rinibar
Hexpath
Islay
Loch Roag
Spinels
Cr#
Mg#
0
10
20
30
40
50
60
70
80
50
55
60
65
70
75
80
85

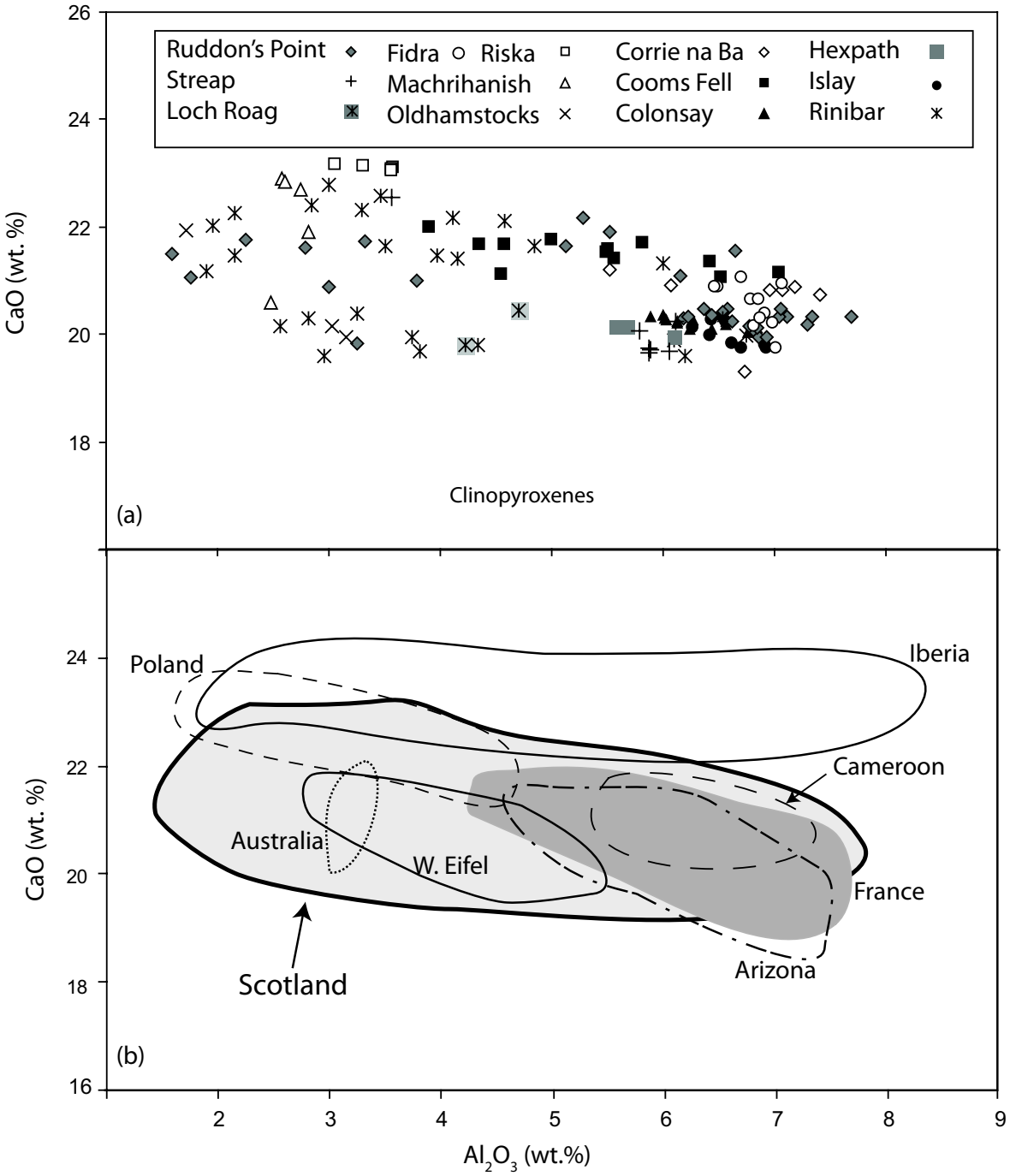
Ruddon's Point
Streap
Loch Roag
Fidra
Riska
Machrihanish
Oldhamstocks
Corrie na Ba
Cooms Fell
Colonsay
Hexpath
Islay
Rinibar
CaO (wt. %)
Clinopyroxenes
(a)
Poland
Iberia
Cameroon
Australia
W. Eifel
France
Arizona
Scotland
(b)
Al_2O_3 (wt.%)

Figure 5.

Figure 6.

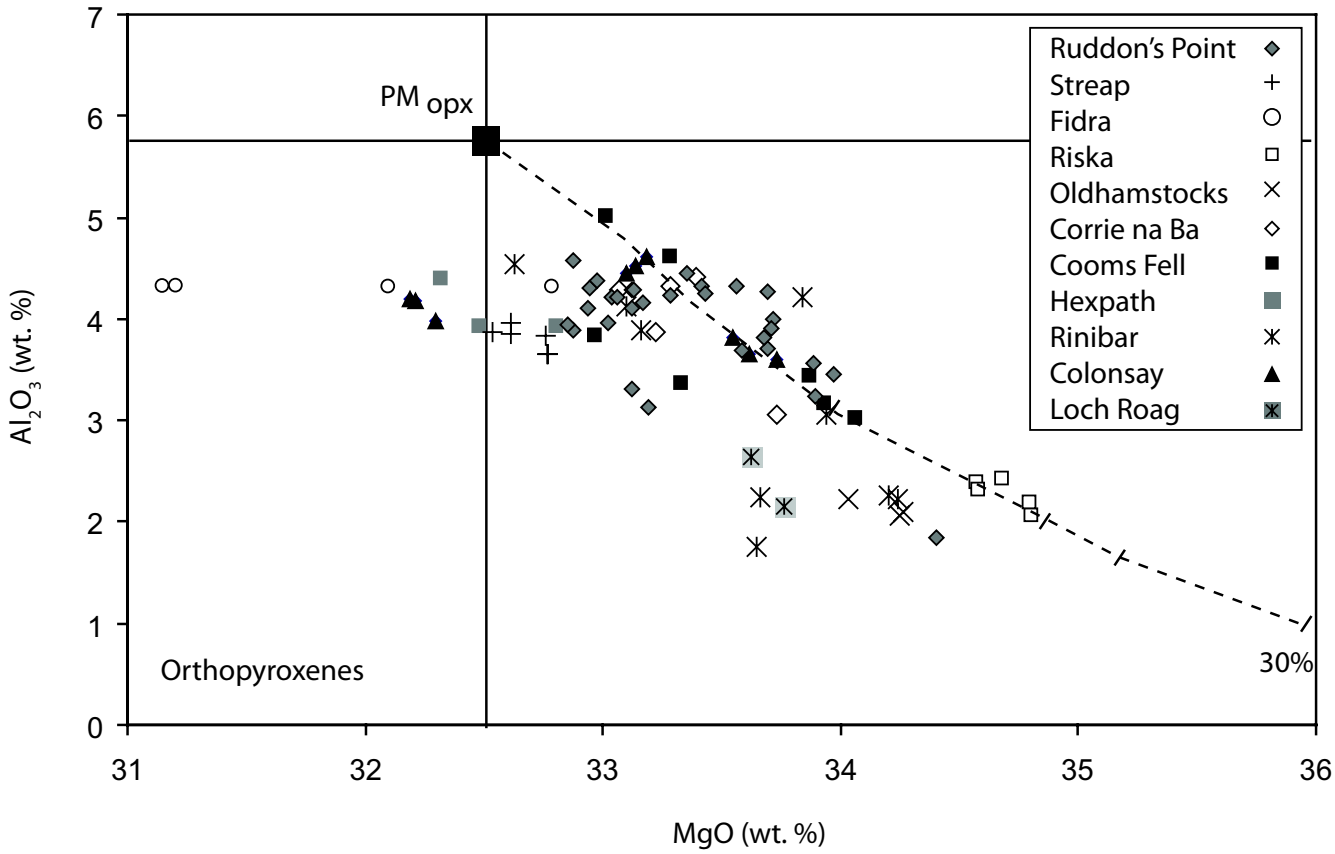
PM opx
Orthopyroxenes
30%
Ruddon's Point
Streap
Fidra
Riska
Oldhamstocks
Corrie na Ba
Cooms Fell
Hexpath
Rinibar
Colonsay
Loch Roag
Al2O3 (wt. %)
MgO (wt. %)
0
1
2
3
4
5
6
7
31
32
33
34
35
36

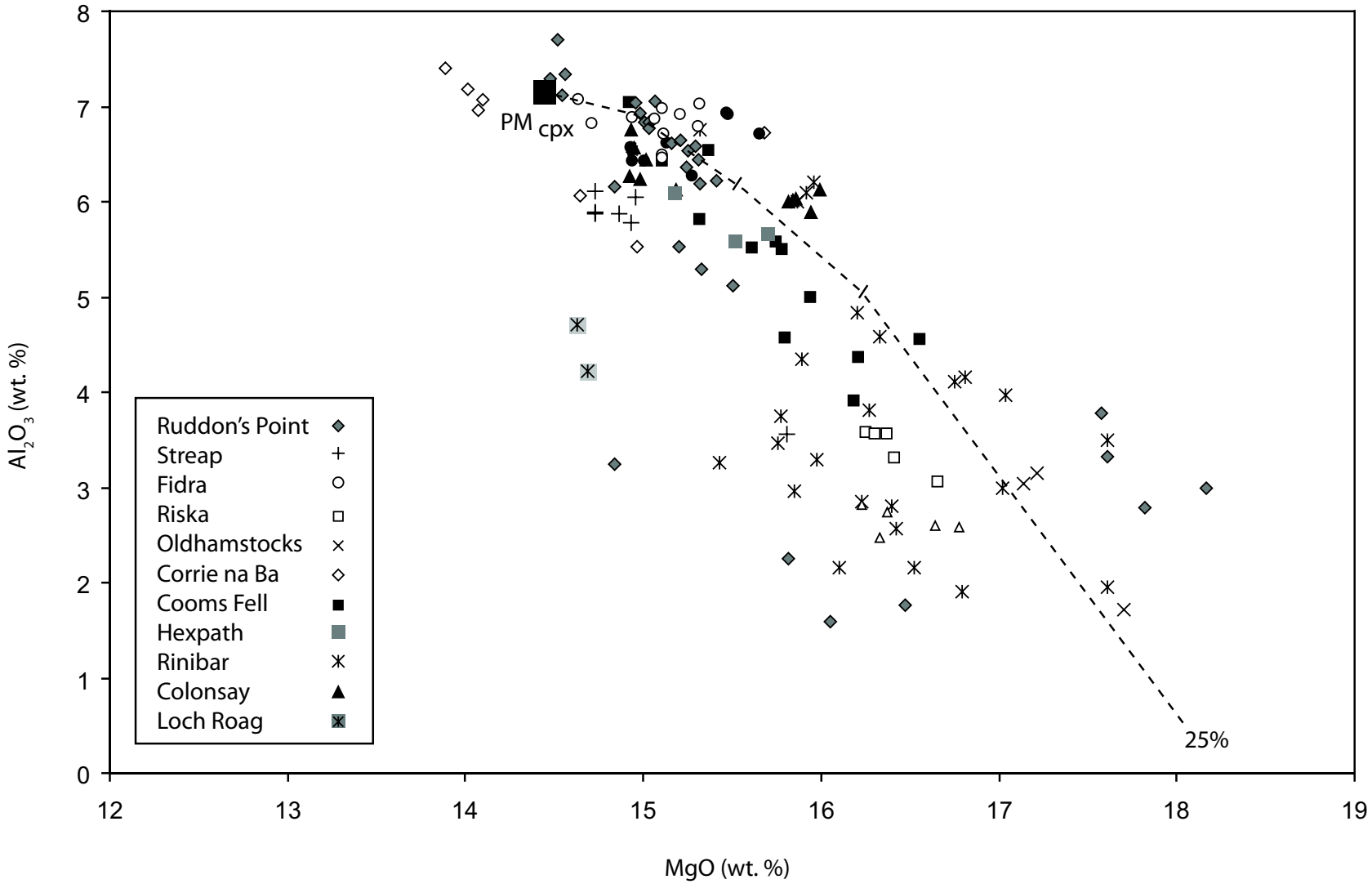
8
7
6
5
4
3
2
1
0
12
13
14
15
16
17
18
19
Al_2O_3 (wt. %)
MgO (wt. %)
PM cpx
25%
Ruddon's Point
Streap
Fidra
Riska
Oldhamstocks
Corrie na Ba
Cooms Fell
Hexpath
Rinibar
Colonsay
Loch Roag

Figure 7.

Figure 8.

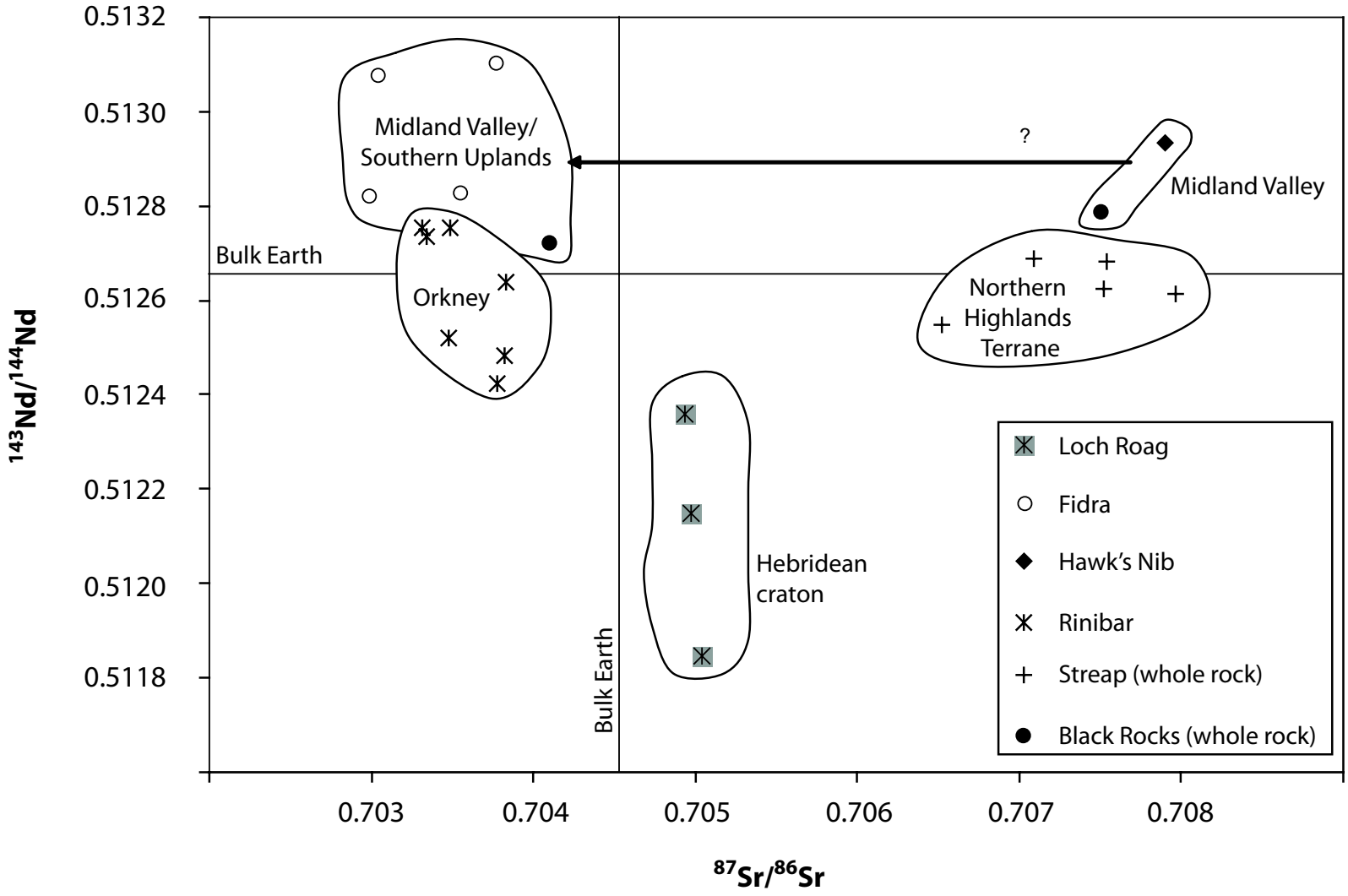
0.5132
0.5130
0.5128
0.5126
0.5124
0.5122
0.5120
0.5118
143Nd/144Nd
Midland Valley/
Southern Uplands
?
Midland Valley
Bulk Earth
Orkney
Northern
Highlands
Terrane
Hebridean
craton
Bulk Earth
Loch Roag
Fidra
Hawk's Nib
Rinibar
Streap (whole rock)
Black Rocks (whole rock)
0.703
0.704
0.705
0.706
0.707
0.708
87Sr/86Sr

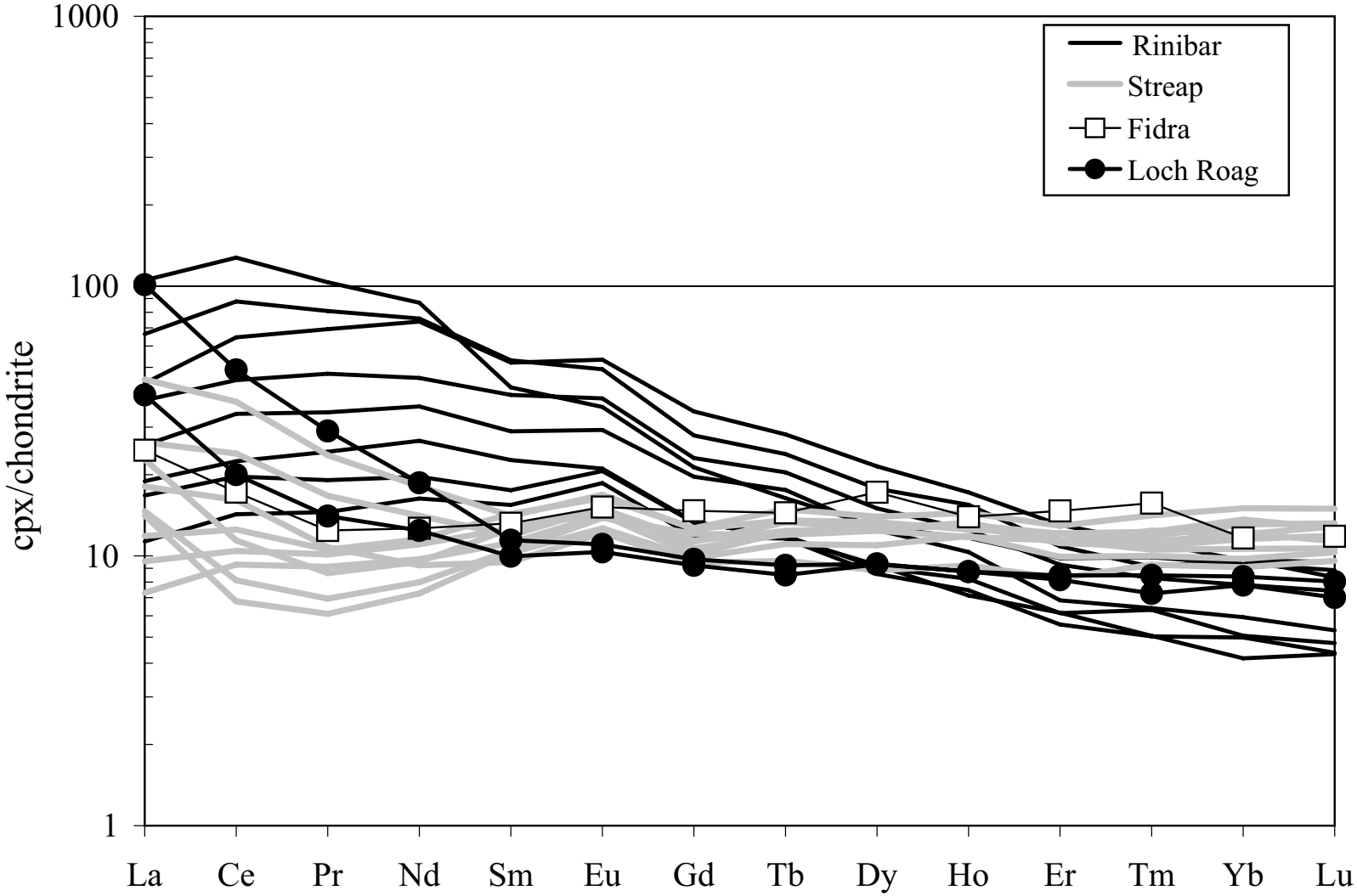
1000
100
10
1
cpx/chondrite
Rinibar
Streap
Fidra
Loch Roag
La
Ce
Pr
Nd
Sm
Eu
Gd
Tb
Dy
Ho
Er
Tm
Yb
Lu

Figure 9.